This is to certify that the

thesis entitled

CHEMILUMINESCENT DETERMINATION OF

AMMONIA BY FLOW-INJECTION ANALYSIS

presented by

Paul Robert Kraus

has been accepted towards fulfillment
of the requirements for

M.S. degree in Chemistry

Major professor

Date 12/9/82

CHEMILUMINESCENT DETERMINATION OF AMMONIA BY FLOW-INJECTION ANALYSIS

By

Paul Robert Kraus

A THESIS

Submitted to
Michigan State University
in partial fulfillment of the requirements
for the degree of

MASTER OF SCIENCE

Department of Chemistry

1982

ABSTRACT

CHEMILUMINESCENT DETERMINATION OF AMMONIA BY FLOW-INJECTION ANALYSIS

By

Paul Robert Kraus

Continuous flow analyses are those processes in which the concentration of an analyte is measured as it flows uninterruptedly through a liquid stream. These techniques are quite flexible and can minimize human intervention in routine analyses. Flow injection analysis is characterized by its mechanical simplicity, high sampling rate, and its adaptability to various types of analyses. A comprehensive theory of flow injection is presented with particular attention to controlling the dispersion of the sample zone. The reaction of ammonia with hypochlorite to form monochloramine has been well documented and has been used in the determination of ammonia. Results are given for the determination of ammonia in river water by the inhibitive effect of ammonia upon the luminol-hypochlorite chemiluminescence reaction. The effect of several interferents upon the analytical results are also presented.

TO MY PARENTS

ACKNOWLEDGMENTS

First and foremost, I would like to express my gratitude to Professor Stan Crouch for his guidance and support throughout the course of this research and thesis preparation. I would also like to thank Professor Andrew Timnick for being my unofficial second reader. It was a real pleasure teaching for you Andy.

A special thanks goes to Chasmo Patton without whom the majority ot this research would no have been possible. Life just won't be the same without Charlie singing the blues, in his own perverse style of course. Gene Ratzlaff was also a great help to me. Thanks for writing the FIA program which enabled be to accumulate my own "HITE REPORT"! That really saved my eyes from hours of staring at chart paper. Gene is the only person I know of who has a digital coffee cup.

I would also like to thank Theresa Fillwock for her faith in me and for helping me to remain somewhat human these past seven months, they've been great Theresa. A big thanks is extended to Dr. Tom Atkinson for creating MULPLT without which the figures in this thesis would not have been possible. I hope that there'll be more "MULPLT WIZARDS" in the future. Lastly, I would like to thank all the friends I've made while here at MSU, your friendship will not be forgotten.

TABLE OF CONTENTS

CHAPTER PAGE

LIST OF FIGURES

FIGURE PAGE

LIST OF TABLES

LIST OF SYMBOLS

a	radial coordinate, mm
C	concentration, mole/liter
C_o^o	concentration of injected sample, mole/liter
C_k	concentration in k^{th} segment after dipersion, mole/liter
C^{max}	concentration of dipersed sample at peak maximum, mole/liter
d_c	helix diameter, mm
d_f	thickness liquid film adjacent to air bubble, mm
d_t	internal diameter of tubing, mm
D	axial dispersion coefficient, cm^2/sec
$D_{w,ss}$	diffusion coefficient of water at 25 °C, dimensionless
D_l	dispersion coefficient, cm^2/sec
D_m	molecular diffusion coefficient, cm^2/sec
Dn	Dean number, dimensionless
D'	dispersion, dimensionless
F	mean linear flow velocity, mm/sec
H	peak height, mm
H_o^o	peak height corresponding to C_o^o, mm
k	segment number
l_i	length of mixing stage, cm
l_s	length of sample zone, cm
L	length of line, cm

L_s	length of liquid segment, cm
M	mass of material injected, mol
n	air segmentation frequency, sec^{-1}
N	number of mixing tanks, dimensionless
q	dispersion parameter, dimensionless
Q	pumping rate, ml/min
r	tube radius, mm
Re	Reynolds number, dimensionless
S	sample volume, µl
t	time, sec
t_i	mean residence time in one tank, sec
T	mean residence time, sec
v(a)	velocity at radial position a, mm/sec
$\langle v \rangle$	mean velocity, mm/sec
V_f	volume of liquid coating tube interior, µl
V_r	reactor volume, µl
V_s	volume of liquid segment, µl
W	peak width at 1/2 peak height, mm
X	distance, cm
δ	dispersion number, dimensionless
γ	surface tension, dyne cm^{-1}
η	solvent viscosity, Poise
ρ	density of solvent, g ml^{-1}

I. INTRODUCTION

Flow injection analysis, as it is known today, was invented simultaneously by two independent groups; Kent Stewart of the United States Department of Agriculture and Jaromir Ruzicka and Elo Hansen of the Technical University of Denmark. Credit for the invention of flow injection is commonly given to Ruzicka and Hansen. In Chapter II a historical outline of the significant advances in flow techniques which have had an influence on the development of flow injection is presented.

By 1978 the theoretical concepts of flow injection were well characterized. Controlling the dispersion of the sample zone is of primary interest in flow injection. The theory of flow injection with particular emphasis on the characterization and manipulation of dispersion is discussed in Chapter III.

The versatility of flow injection is demonstrated in this thesis by the chemiluminescent determination of ammonia. The chemistry involved in this system can be broken into two parts: the first involves the reaction of ammonia with hypochlorite in alkaline solution to form monochloramine. The excess hypochlorite will react with luminol to yield chemiluminescence. Monochloramine does not produce chemiluminescence with luminol. The kinetics of these two mechanisms is presented in Chapter IV.

To determine the applicability of this system to a real sample the effect of sixteen interferents on the chemiluminescence is investigated. River water from the Red Cedar River was analyzed for ammonia using this proposed system. The sample was also analyzed by a standard method and the two results are compared.

II. HISTORICAL

A. Continuous Flow Analysis

Continuous flow analysis (CFA) refers to a process in which the concentration of an analyte is measured uninterruptedly in a stream consisting of either a liquid or a gas. Samples successively pass through the manifold (that part of the system between the pump and the detector) where reagents are added at strategic points. Mixing and incubation take place while the sample solution is on its way to the detector, where the signal is continuously monitored and recorded. Typical detection systems. are ion-selective eletrodes or spectrophotometry with flow-through cuvettes. Early systems had the problem of considerable intermixing of adjacent samples during their passage through the manifold. In 1957 Leonard Skeggs [1] introduced the concept of segmenting the sample stream with air bubbles to prevent excessive dispersion of the sample by the natural dispersive nature of laminar flow. The air bubbles divided the flowing stream into a number of compartments and therefore prevented excessive dilution of the sample. The reaction time was determined by the length, the inner diameter and the flow rate of the manifold conduit. Just prior to the detector the air bubbles were removed from the sample stream, and the resulting non-segmented stream passed through the flow cell of a colorimeter. The detector response was recorded, and the peak height

was measured to determine the concentration of the analyte. This system was originally designed by Skeggs for the determination of urea and glucose in blood and is shown in Figure 1. The system worked with a sampling rate of up to 40 samples per hour with good precision. Skeggs' system was later developed by Technicon Corp. and marketed as the AutoAnalyser.

The continuous flow approach is a very flexible method to perform many necessary operations in a chemical analysis. Aside from operations which are executed by a batch analyzer, such as sample dispensing, dilution, heating, mixing, and reagent additon, the continuous flow analyzer also has the capability to perform dialysis, distillation, solvent extraction, and other methods of separation. In a CFA system it is the liquid that is in motion and therefore the instrument has fewer moving parts which makes it mechanically less complex and easier to construct than a batch analyzer [2].

FLOW INJECTION ANALYSIS

The air segmented continuous-flow analyzer works well for relatively low rates of analysis (10-30 samples/hour). However, baseline readings are not attained at higher rates (over 60 samples/hour) of analysis and there is also considerable loss of precision. The first use of nonsegmented continuously flowing streams can be traced back to 1958 when Spackman, Stein, and Moore [3] described the first semiautomated amino-acid analyzer which was the prototype of the modern high-performance liquid chromatographic system. The effluent stream was mixed with reagent after the ion-exchange

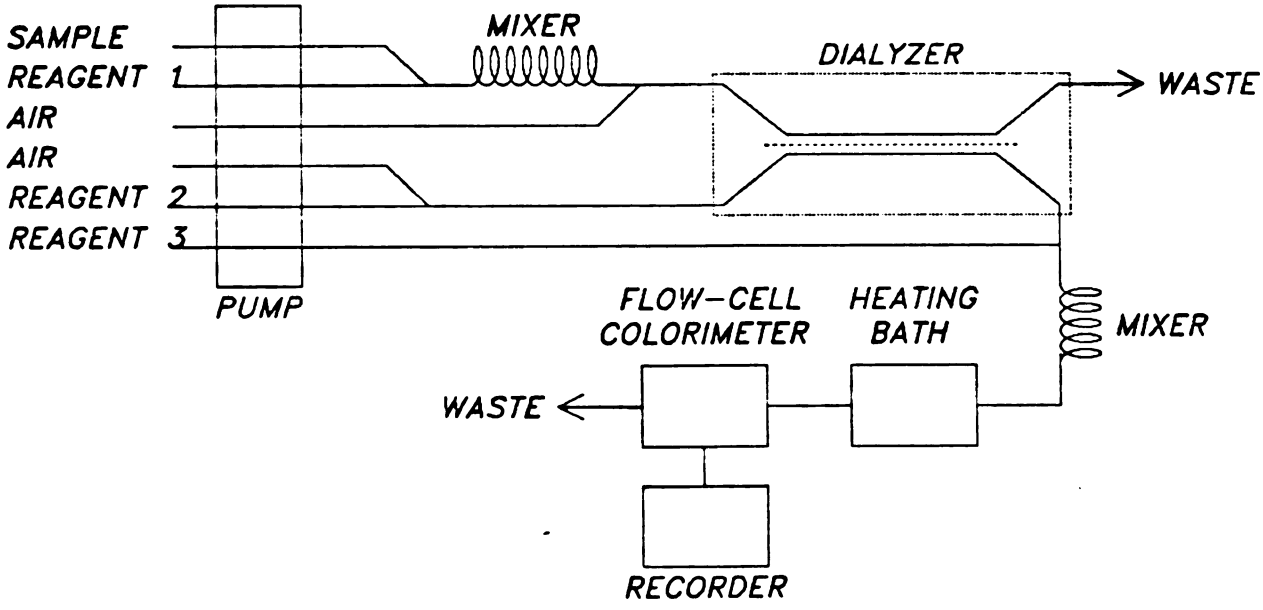

Figure 1. Flow diagram of Skeggs' urea and glucose analyzer.

column, and the eluent mixture flowed through 95 ft of 0.7 mm Teflon tubing which was immersed in boiling water. At the end of this reaction bath the solution entered a small tube attached to the bottom of the flow-cell in the colorimeter where the solution flowed up through the flow-cell and to a constant-head waste tube. The colorimeter output was monitored on a strip-chart recorder and the concentrations of the amino-acids were determined by measuring the area under each peak. This first use of a nonsegmented continuously flowing stream for discrete sample analysis, the use of fine capillary conduit, area measurement for the determination of analyte concentration, and the use of a positive diplacement pump to propel the reagents are the innovations that led to the development of Flow Injection Analysis (FIA).

The earliest report of what may be called FIA was in 1970 when Nagy, Feher, and Pungor [4] used graphite electrodes for the voltammetric measurement of samples injected into a nonsegmented continuously flowing stream with a hypodermic needle. The sample and carrier stream were mixed in a small mixer and the response was measured downstream with a flow-through electrode.

Several papers appeared in 1972 which provided some critical concepts for FIA. Bergmeyer and Hagen [5] described a new principle for the enzymatic analysis in which dissolved glucose samples were injected into a nonsegmented stream of recirculated buffer which then passed through a small chamber containing bound glucose oxidase and past an oxygen electrode. The response of the electrode was then recorded on a strip-chart recorder. According to Kent Stewart this is the first use of FIA for enzymatic analysis [6].

Also in 1972, White and Fitzgerald [7] determined ascorbic acid by the photobleaching of the ascorbic acid-Methylene Blue complex in a continuously flowing stream. Even though the manifold was of a larger diameter than normally used in FIA they did develop conditions in which they could inject discrete 1 ml samples every 1-2 minutes.

Another significant contribution was made by Gerding, Kemper, Lamers, and Gerding [8] who devised a sensitive detection system for peptides and proteins in column effluents. They used a nonsegmented continuous-flow system with small diameter manifolds (0.3 mm inner diameter). Very slow delivery syringe pumps (1 ml/hour) were employed, and a system of valves was used with two sample loops to transfer samples from the chromatographic effluent stream to the reaction stream while maintaining flow in each channel. This was the first realization that if very small inner diameter tubing is used at a slow pumping rate air-segmentation is not required to maintain sample integrity.

Frantz and Hare [9] described a nonsegmented continuous-flow system for the determination of silica in 1973. Reagent was pumped through the manifold (40 ft. of 0.2 mm Teflon tubing) by a pressurized chamber. Sample injection was achieved by inserting a micro-pipette into the flowing stream of reagent. In order that the sample injection system be by-passed while pipettes were changed, the insertion of the pipette was accomplished by using two three-way valves. The flow-cell was used in a special colorimeter [10] with an inner diameter of 0.5 mm and a path length of either 6 or 60 mm. In this system are inherent all of the fundamental concepts of FIA as it is described today.

In 1974 Feher and Pungor [11] modified the apparatus used in their 1970 work and used peristaltic pumps, Hamilton syringes, and the dropping mercury electrode. They had used flow rates of 5-8 ml/min which is more typical of today's FIA systems. The concentration of the analyte injected into the system was found to be proportional to the sample peak area, and the signal responses were a linear function of the analyte concentration.

In 1975 two parties simultaneously, but independently, developed a flow system which would maintain sample integrity without air segmentation. Kent K Stewart [12] approached the problem from the standpoint of liquid chromatography and Jaromir Ruzicka and Elo Hansen [13] approached the problem as nonsegmented continuous flow. These early FIA systems are shown diagrammatically in Figures 2. and 3. respectively. Ruzicka and Hansen coined the name Flow Injection to describe this particular method of analysis and it is for this reason they are given credit for inventing FIA.

The system used by Stewart, Beecher, and Hare [12] consisted of a sample flow system which carried the sample solution and wash solution, segmented by air, and a reaction flow system in which the sample was analyzed. Samples were injected into the reaction flow system by a stream sampling valve which removed a fixed volume of sample without air contamination from the sample stream. The manifold conduits were 0.25 mm i.d. Teflon tubing. Sampling rates of 120 samples per hour were obtained with complete washout between samples (complete return to baseline of colorimeter output).

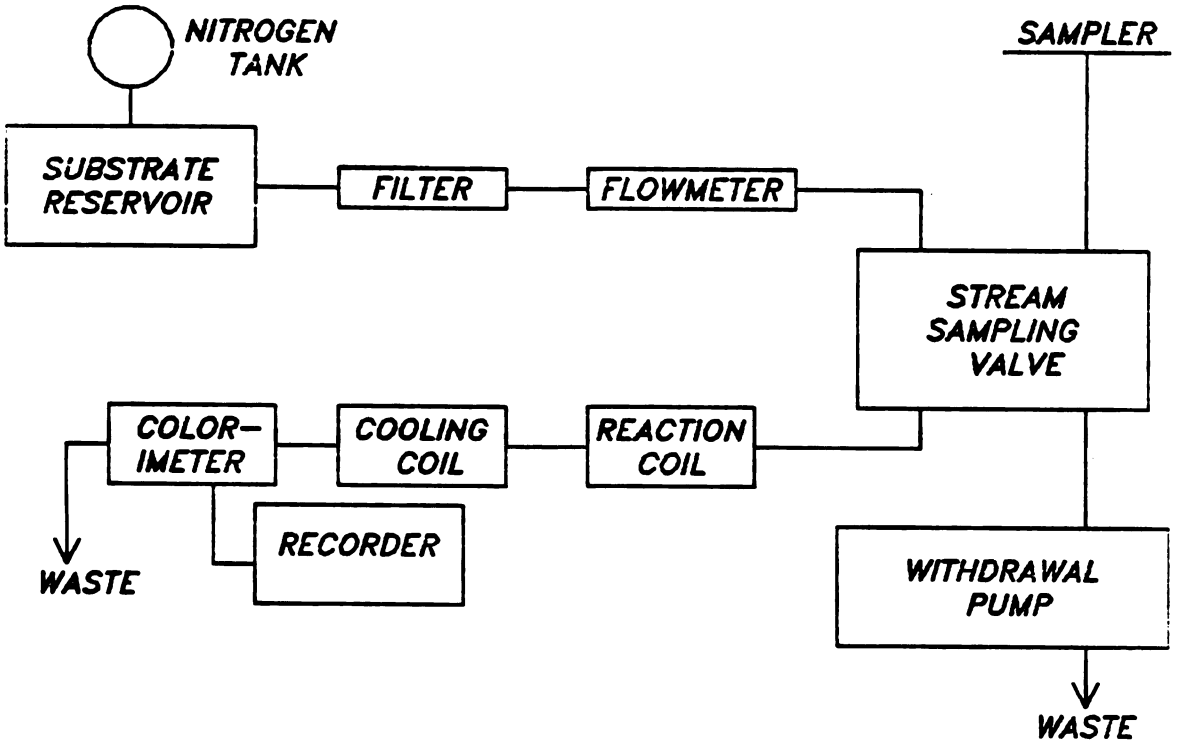

Figure 2. **Schematic diagram of Stewart's FIA system.**

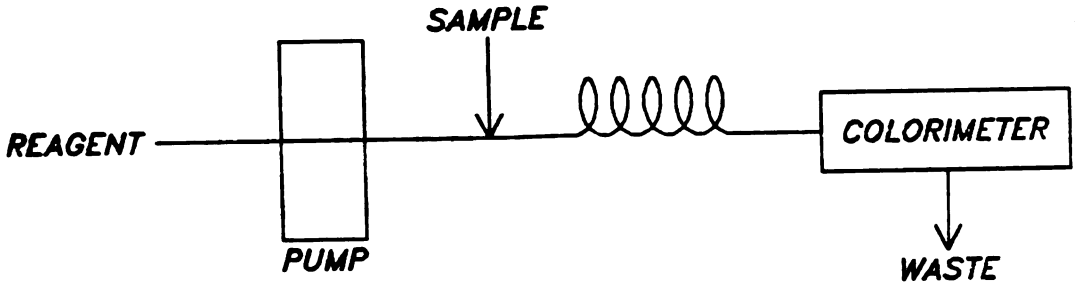

Figure 3. **Manifold used in Ruzicka and Hansen's first FIA experiments.**

In their first paper of a series of ten, Ruzicka and Hansen [13] illustrated the concepts of FIA by the colorimetric determination of methyl orange. They had injected the yellow basic form of the indicator into an acidic carrier stream. This acidic carrier not only provided the transport but also served as the color development reagent. Their system had a pumping rate of 18 ml/min with a 0.50 ml sample volume. The sample was manually injected into the flow stream with a syringe. With this manual injection technique the maximum sampling rate was approximately 270 samples per hour with no carry-over between samples. The second paper of the series [14] described efforts to further describe such parameters as sample volume, tube diameter, and tube length so that the limitations of FIA could be better understood.

By 1976 the number of papers being published on FIA had greatly increased, and all of the fundamental concepts of had been developed. The remaining papers in the series by Ruzicka and Hansen describe various types of analyses with increasingly complex manifolds [15-21]. The final paper of the series [22] is a review of the theory, techniques and trends of FIA.

III. THEORY of FIA and CFA

Flow-injection analysis involves the injection of a small, but precisely known, volume of sample into a continuously flowing stream of reagent. The sample/reagent solution is mixed in the manifold, and the analyte in its desired form is measured downstream by a flow-through type detector. Due to the absence of air-segmentation, the apparatus used for FIA is considerably less complex than that used in CFA. A FIA system is easy to construct, easy to modify, and as a result it lends itself to many novel applications. Because of its speed, simplicity, and economy there are authors [23] who believe that FIA will eventually replace CFA in many clinical chemical analyses. FIA, as Ruzicka and Hansen [22] have described is based upon three principles: (a) sample injection, (b) controlled dispersion, and (c) reproducible timing.

SAMPLE INJECTION

Sample injection involves placing a well-defined sample zone into a continuously moving carrier stream such that the flow of the stream is not disturbed. The exact volume of the sample that is injected does not need to be known, but it must be introduced into the carrier stream precisely such that the volume and the length of the sample slug are reproduced from one injection to the next. This method of sample introduction is more precise than the timed aspiration technique normally used in CFA. The injector used by Stewart *et al.* [12] is a

pneumatically actuated stream sampling valve as is shown in Figure 4. This type of valve removes a fixed portion of the sample from the sample flow system and introduces it into the reaction flow system. Samples were aspirated through the sample channel of the valve from a sample cup in a standard sampler. After a set period of time the sample probe moved from the sample cup to the wash cup and then to the next sample cup. While the sample probe is moving from one cup to the next a small amount of air is introduced into the sample stream. The stream-sampling valve was timed to the sampler so that a portion of the sample stream that is not contaminated by air is injected into the reagent stream. With this system of injection discrete sample slugs are placed into the reagent stream.

The first injection technique used by Ruzicka and Hansen [13] is somewhat more primitive. Samples were injected manually from syringes. Their early experiments were performed with an injector made of a rubber tube situated in a perspex block with precisely bored holes; controlled piercing of the rubber tube by the hypodermic needle was used. The tube had the problem of bleeding after multiple injections. Thus a subsequent injection block was made of two perspex blocks screwed together with a silicone rubber disk (from a Gas Chromatograph injection port) squeezed between the two blocks to serve as a septum. This system proved to be more durable and is shown in Figure 5. The needle guide was designed so that the orifice of the inserted hypodermic needle was situated in the carrier stream for injection. In part three of their FIA series Ruzicka and Hansen [15] changed to a simple flap valve which is shown in Figure 6. During an injection the pressure of the sample being injected opened the flap and allowed the

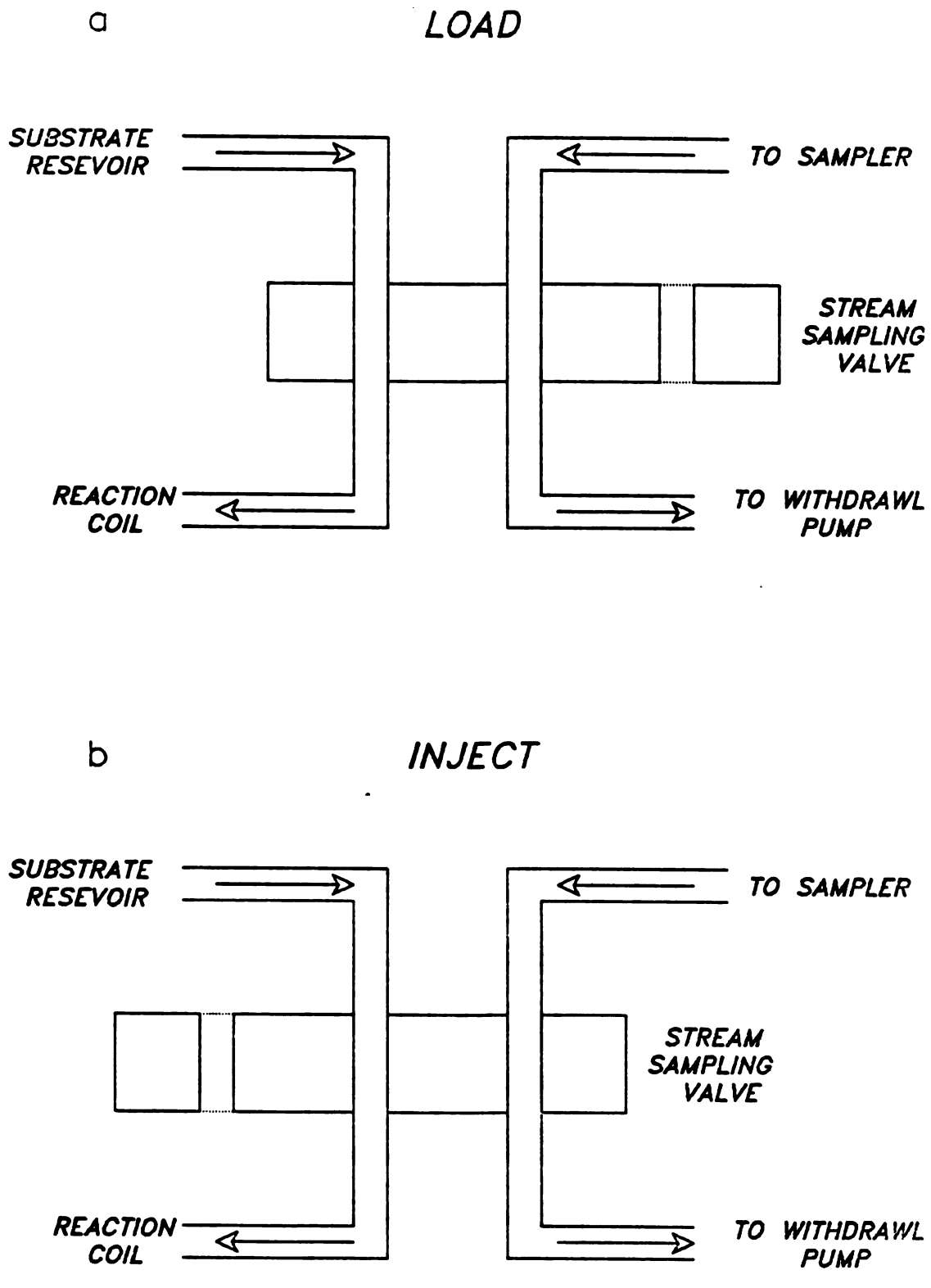

Figure 4. **Stream Sampling valve used by Stewart et al. shown in the (a) load and (b) inject positions.**

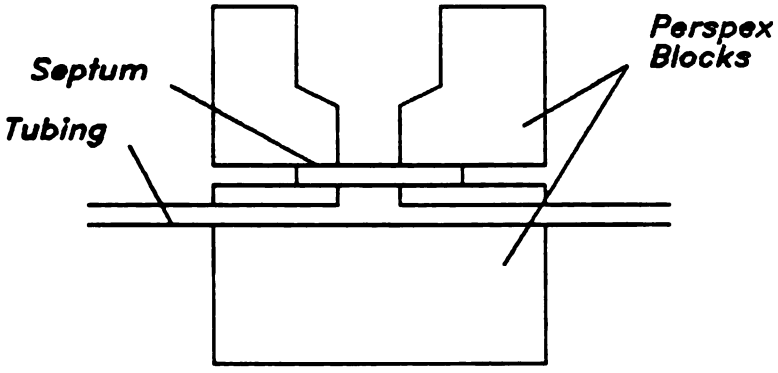

Figure 5. Injector block.

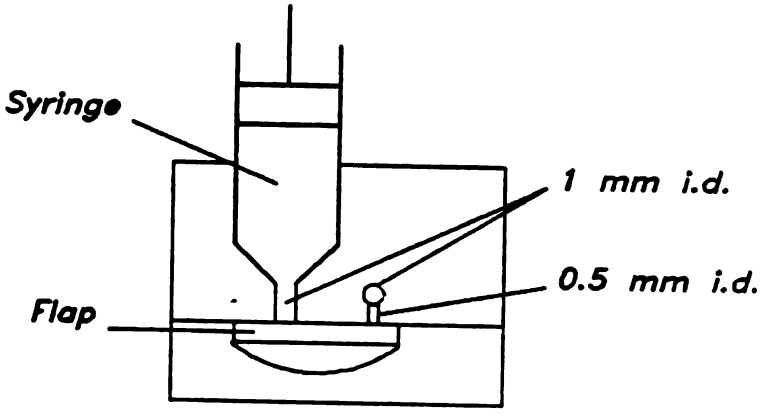

Figure 6. Flap valve.

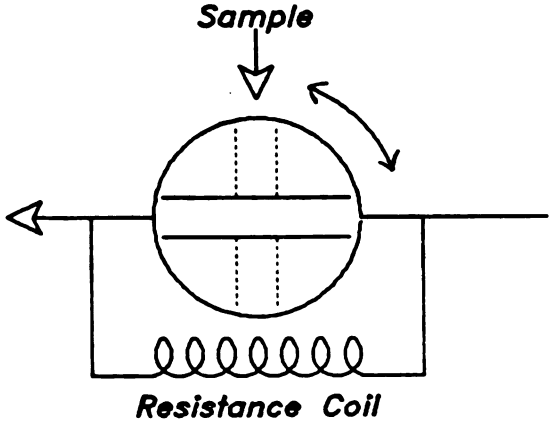

Figure 7. Rotary sample injection valve with bypass coil shown in the inject position.

sample to enter the carrier stream. Although this technique was simpler to use and had a dead volume of less than 3 µl, it was still a manual technique. Inherent in these manual injection techniques is a sudden surging of the carrier stream as the sample is injected. This disruption of the flow causes a momentary difference in the mixing ratios at the points in the manifold where two streams meet. In order to minimize this sudden pulsation an injection pulse dampener was designed by Bergamin, Reis, and Zagatto [24].

By the sixth paper of their series Ruzicka and Hansen [18] had devised the semi-automated sample injector shown in Figure 7. This system has the advantage of having a higher degree of precision for sample volumes being injected. It is also capable of injecting a wide range of volumes by simply changing the volume of the sampling loop. While the sample loop is being "loaded" the carrier stream bypasses the valve through a coil of high flow resistance. When the valve is switched to the "inject" position the carrier stream passes through the sample loop which has a lower flow resistance. The bypass coil also serves to dampen the sudden surge created by the switching of the valve. More recently, chromatographic valves which are able to deliver very small sample volumes have been used [25].

One disadvantage of all continuous-flow systems is the reagent consumption which occurs when there is no sample present in the apparatus. This poses no real problem when the reagents are inexpensive, but can become quite uneconomical when an expensive reagent or an enzyme is used. In order to overcome this unnecessary waste of solutions the Merging Zones principle was developed and can be achieved in two ways: intermittent pumping [26], or through the use of

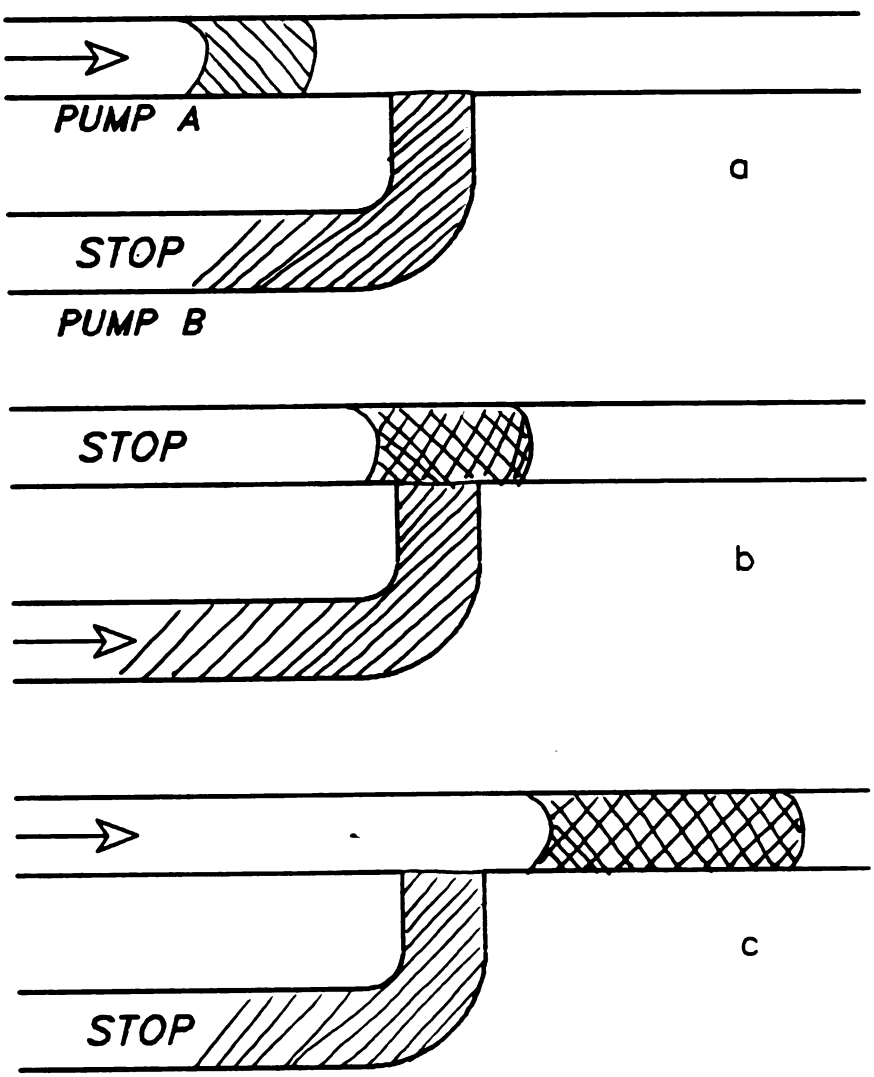

Figure 8. Merging zones with intermittent pumping: (a) pump A moves injected sample slug to merging zone, (b) with slug at merging zone pump A is turned off and pump B is activated to deliver reagent, (c) pump A is now reactivated.

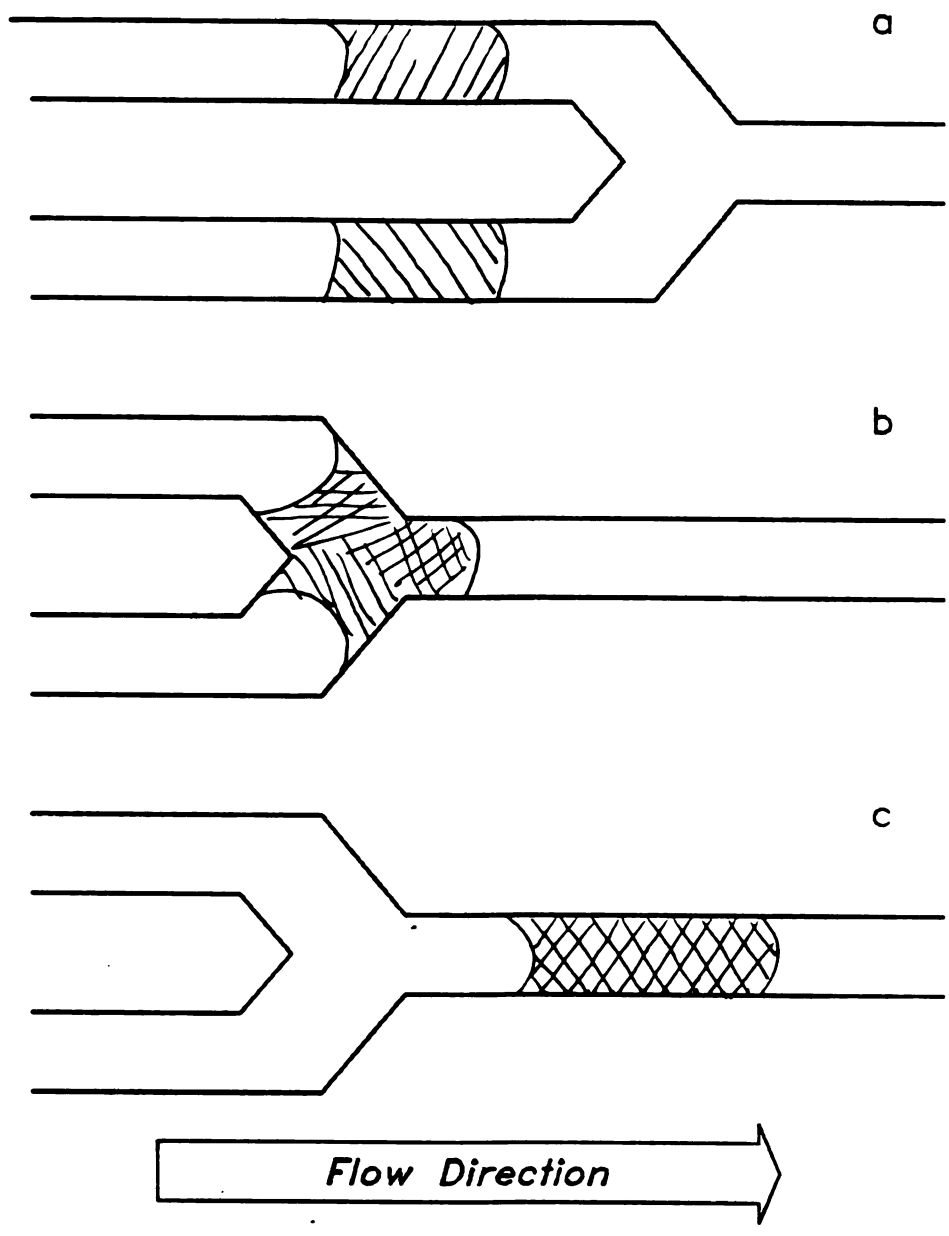

Figure 9. **Merging zones with multiple injection valves: (a) sample and reagent are injected into a carrier stream and mix at the merging point (b), (c) sample and reagent mix in manifold.**

a multiple injection valve [27] (see Figures 8. and 9, respectively). What both these methods have in common is that the carrier stream is no longer the reagent, but rather it is distilled water or a suitable buffer.

Intermittent pumping requires the use of two pumps. Sample is injected into a stream controlled by pump A. When the sample zone reaches the merging point, pump A is turned-off and pump B, which controls the reagent stream, is turned-on. Once a predetermined amount of reagent has been added, pump B is turned-off and pump A is turned-on. This method allows the amount of reagent added to be regulated by the length of time pump B is operating.

The multiple injection valve requires two valves, one to inject the sample and the other to inject the reagent into two separate carrier streams each pumped at the same rate. The sample and reagent slugs mix when the respective streams meet at the merging point. Both of these techniques require precise timing, but there can be a considerable conservation of reagent compared to filling the entire manifold.

SAMPLE DISPERSION

It was first observed by Sir Isaac Newton that when water flowed slowly and steadily through a pipe a longitudinal velocity profile was established by the frictional forces between the layers of moving liquid. This condition of laminar flow is characterized by having the velocity of the axially centered liquid twice that of the mean velocity and the velocity of the liquid layer in contact with the tube surface being practically stationary. This can be expressed mathematically by

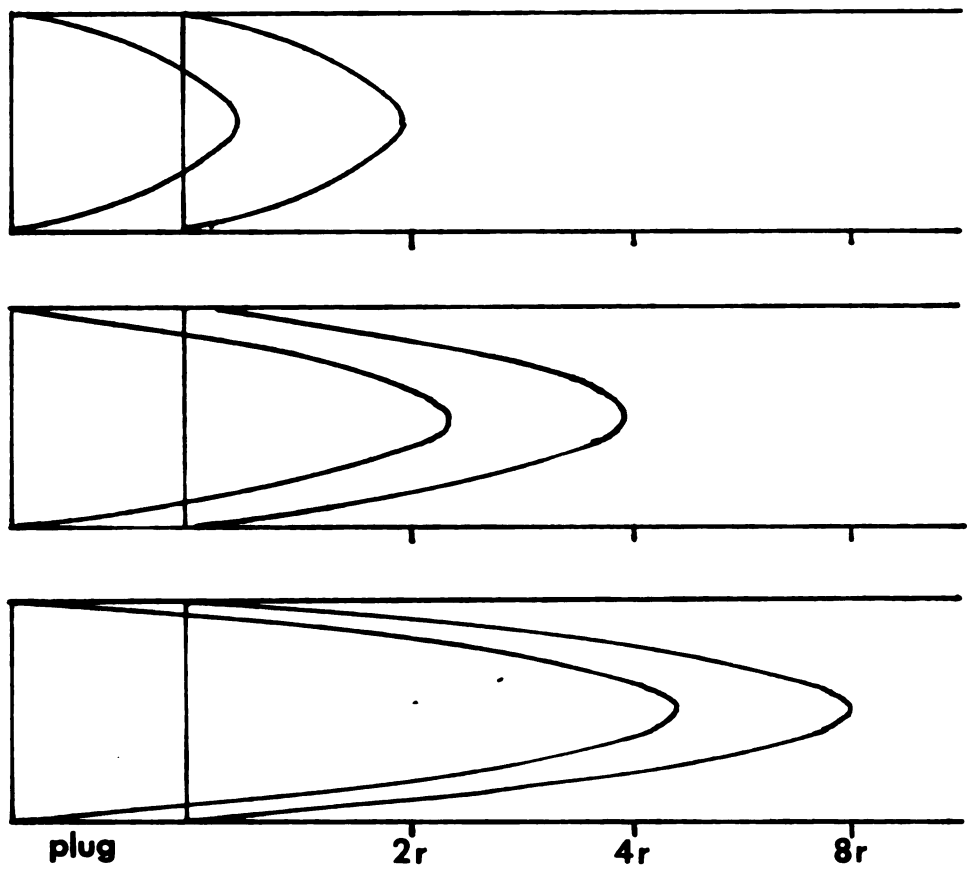

Figure 10. Distribution of sample plug at various times after injection. Without molecular diffusion an infinite tail is obtained.

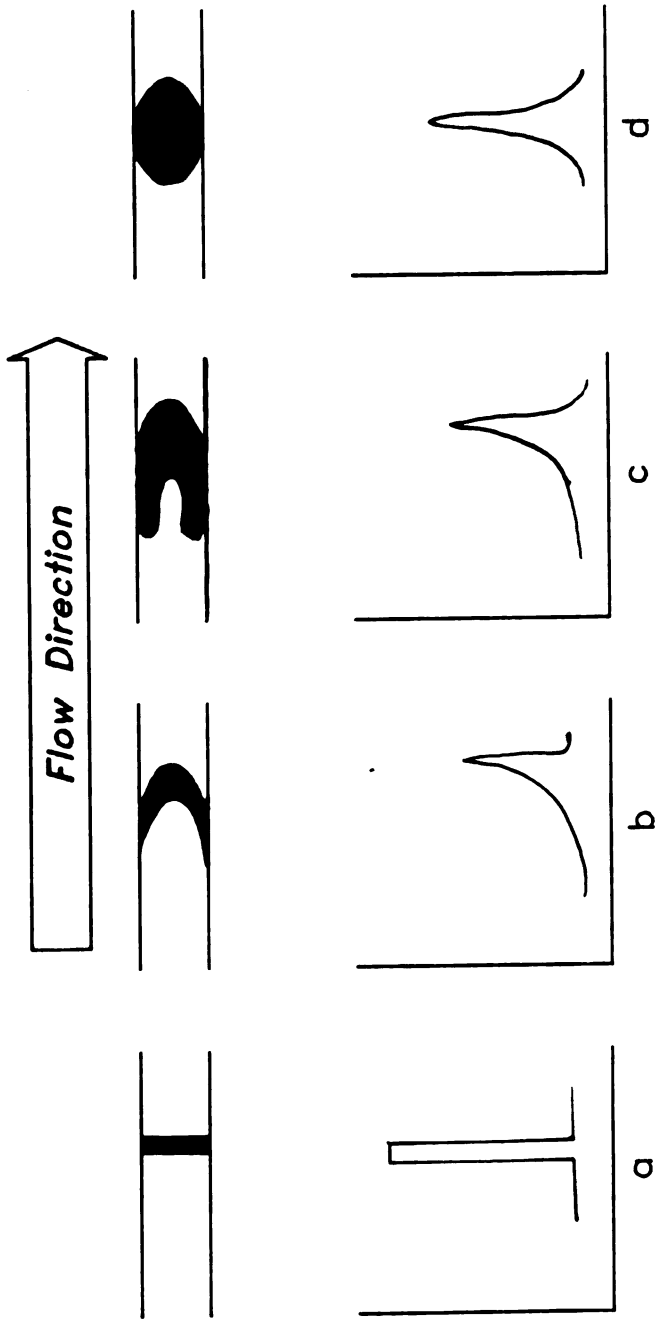

Figure 11. Laminar flow with molecular diffusion: (a) the sample plug, (b) under conditions of laminar flow, (c) laminar flow with molecular diffusion, (d) Gaussian profile resulting from molecular diffusion.

Equation (1),

$$v(a)=2\langle v\rangle(1-a^2/r^2) \qquad (1)$$

where v(a) is the velocity (mm/sec) at radial position a (mm), $\langle v\rangle$ is the mean velocity (mm/sec), and r is the tube radius. This is shown in Figure 10. The sample is injected into the carrier as a plug; the movement of the carrier stream together with laminar flow cause the sample plug to adopt a parabolic velocity profile. Without molecular diffusion the sample would have an infinite tail; the leading edge of the sample would be in the detector and the trailing edge would still be in the injector. This would result in an entirely unacceptable carryover between samples. Fortunately, molecular diffusion between the sample and the carrier results in radial diffusion which is perpendicular to the direction of flow. Therefore, sample molecules on the leading edge, which are axially centered in the tube, tend to diffuse radially toward the tube surface, and the sample molecules at the trailing edge diffuse toward the center of the tube. The concentration profile of the sample zone broadens out as it moves downstream. Figure 11. shows the profile of the sample zone under various conditions. In (a) the plug is shown. In (b) the zone is shown under the condition of laminar flow which is asymmetrical. In (c) laminar flow and molecular diffusion have produced a more symmetrical profile. Finally, the Gaussian profile resulting principally from molecular diffusion is shown in (d).

Changing flow parameters allows the dispersion to be manipulated to suit the particular requirements of a desired analytical procedure. Dispersion of the sample zone has been categorized as either limited, when the original composition of the sample is to be measured (the

center of the sample zone remains intact), medium, when the entire sample zone must be mixed with the carrier reagent so that a reaction can occur, and large, where the concentration profile between the sample plug and the carrier stream is to be measured [22]. Figure 12. shows the characteristic manifolds used to obtain the corresponding dispersion types. The dispersion numbers given in Figure 12. are discussed later. Dispersion is dependent on the flow velocity. Under the conditions of laminar flow, axial despersion is due to the velocity gradients (see Equation (1)). However, if the flow rate is increased, laminar flow is replaced by turbulent flow which is characterized by the chaotic movement of the sample and reagent molecules in all directions being equal. The onset of turbulence is given by a Reynolds number Re greater than 1000 where

$$Re=4\rho Q/(\pi d_t \eta) \qquad (2)$$

or for dilute aqueous solutions

$$Re=21.2Q/(2r) \qquad (3)$$

where ρ is the density of the solvent, Q is the pumping rate (ml/min), d_t is the tube diameter (mm), and η is the solvent viscosity. Although it was originally thought that FIA operated under conditions of turbulent flow [13], it can be seen from Equation (3) that in a manifold of 1 mm internal diameter, a volumetric pumping rate of 93 ml/min is required to reach conditions of turbulent flow. This is a highly uneconomical pumping rate from the standpoint of reagent consumption.

Operating at lower pumping rates causes mixing to be a result of molecular diffusion. Taylor [28] was the first to describe this process and described it mathematically in the "Taylor Equation",

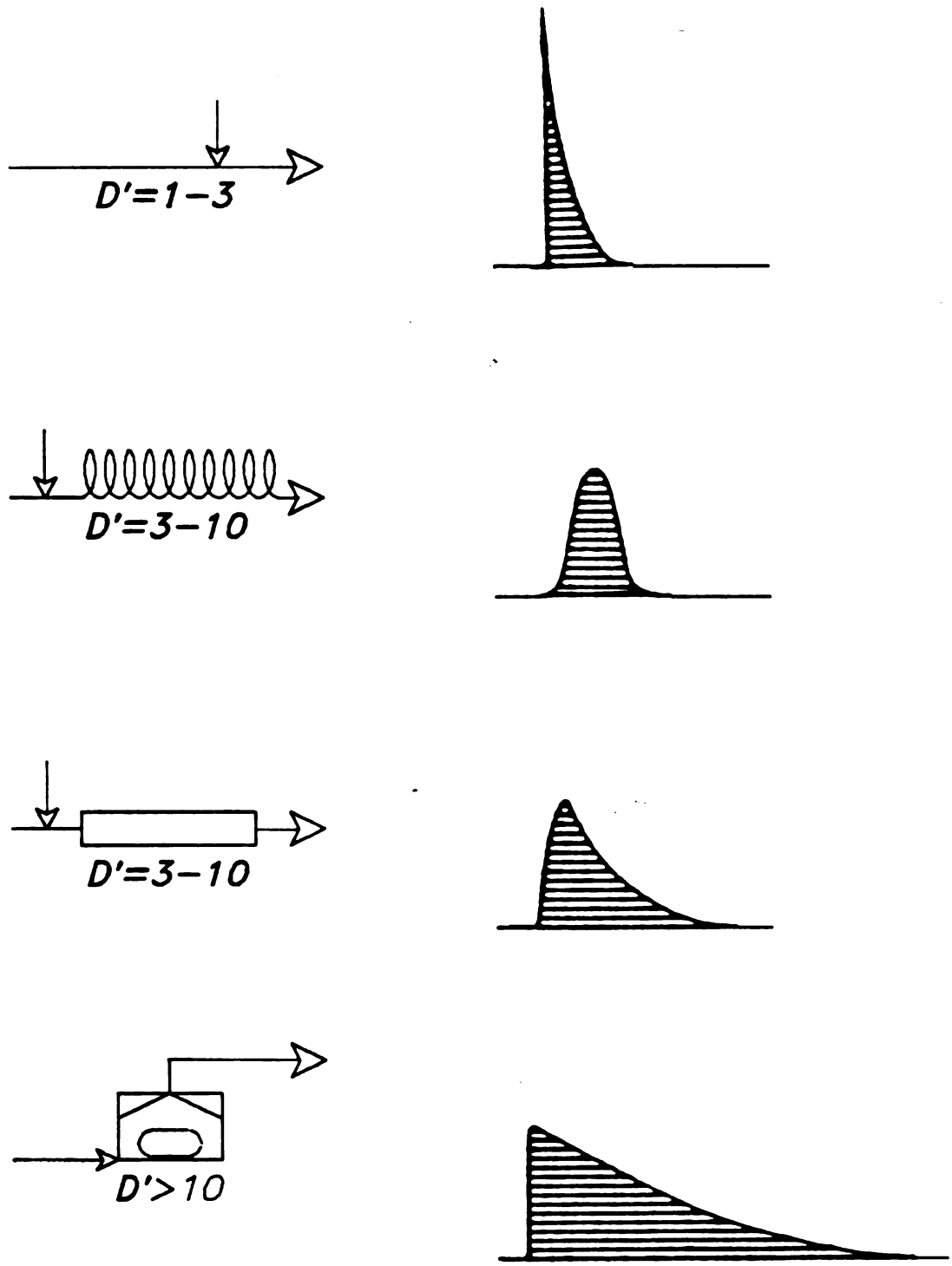

Figure 12. Common manifold designs used in FIA with their characteristic concentration profiles.

$$C = M \frac{1}{r^2 \pi} \left(\frac{1}{2(\pi \delta L^2)^{1/2}} \quad e^{-(L-X)^2/L^2 4\delta} \right) \tag{4}$$

where C is the concentration at point X, M is the mass of the sample injected, r is the tube radius, and

$$\delta = Dt/L^2. \tag{5}$$

Equation (4) shows that under conditions of laminar flow the dispersion increases with the square of the tube radius. From Equation (4) and from the dependence of dispersion on the flow rate [29],

$$D_L = D_m + \left[d_t^2 \langle v \rangle^2 / 192 D_m \right] \tag{6}$$

where D_L is the dispersion coefficient and D_m is the molecular diffusion coefficient, it can be seen that decreasing the flow rate in narrow tubes results in a decrease in the dispersion.

The type of the manifold used also has an effect on the amount of dispersion obtained, and hence, the shape of the concentration curve (C-curve) obtained. One model for describing the flow geometry is the tank-in-series model which is based on the idea that the manifold can be thought of as a series of mixing tanks all of equal size which are analogous to the plates of a chromatographic column. The normalized C-curve follows the equation [30],

$$C = (1/t_i)(t/t_i)^{N-1} \frac{1}{(N-1)!} e^{(-t/t_i)} \tag{7}$$

for any number of tanks which reduces to

$$C = (1/t_i) e^{(-t/t_i)} \tag{8}$$

for one tank, where N is the number of tanks and t_i is the mean residence time of the solution in one tank. For a very large N the curve approaches a Gaussian shape and as N decreases the peaks become increasingly asymmetrical. The C-curves for N=1,2,3,4,5 are shown in

Figure 13. From Figure 13. it is easy to see that symmetrical gradient profiles are obtained in long narrow tubes which accommodate a large number of identical mixing stages. It is obvious that the easiest way to increase the number of mixing tanks, and hence the residence time T, is to increase the line length L since

$$N=L/l_i \tag{9}$$

where l_i is the length of a single mixing stage. The residence time and line length are related through the pumping rate Q or linear velocity F:

$$QT=\pi r^2 L=QL/F=V_r. \tag{10}$$

Although this equation only applies for a single line manifold of a uniform diameter, the residence time of the sample is easy to measure since it coincides with the time taken from the injection until the peak maximum appears on the detector.

With the exception of gradient techniques, where the concentration profile within the sample zone is the area of interest, a rigorous approach to the design and description of Flow Injection systems is not necessary. For cases where the analytical readout is based on the peak height, the dispersion D' can be defined as the ratio of the concentrations before and after the dispersion has occurred,

$$D'=C_o^o/C^{max}=const'H_o^o/const''H. \tag{11}$$

The concentration of the injected sample solution is C_o^o, C^{max} represents the concentration of the dispersed sample at the peak maximum, H_o^o is the peak height corresponding to a flow-cell filled with a solution with concentration of C_o^o, and H is the peak height corresponding to a sample concentration of C^{max}. The conversion factors between instrument readout and the concentration are const' and

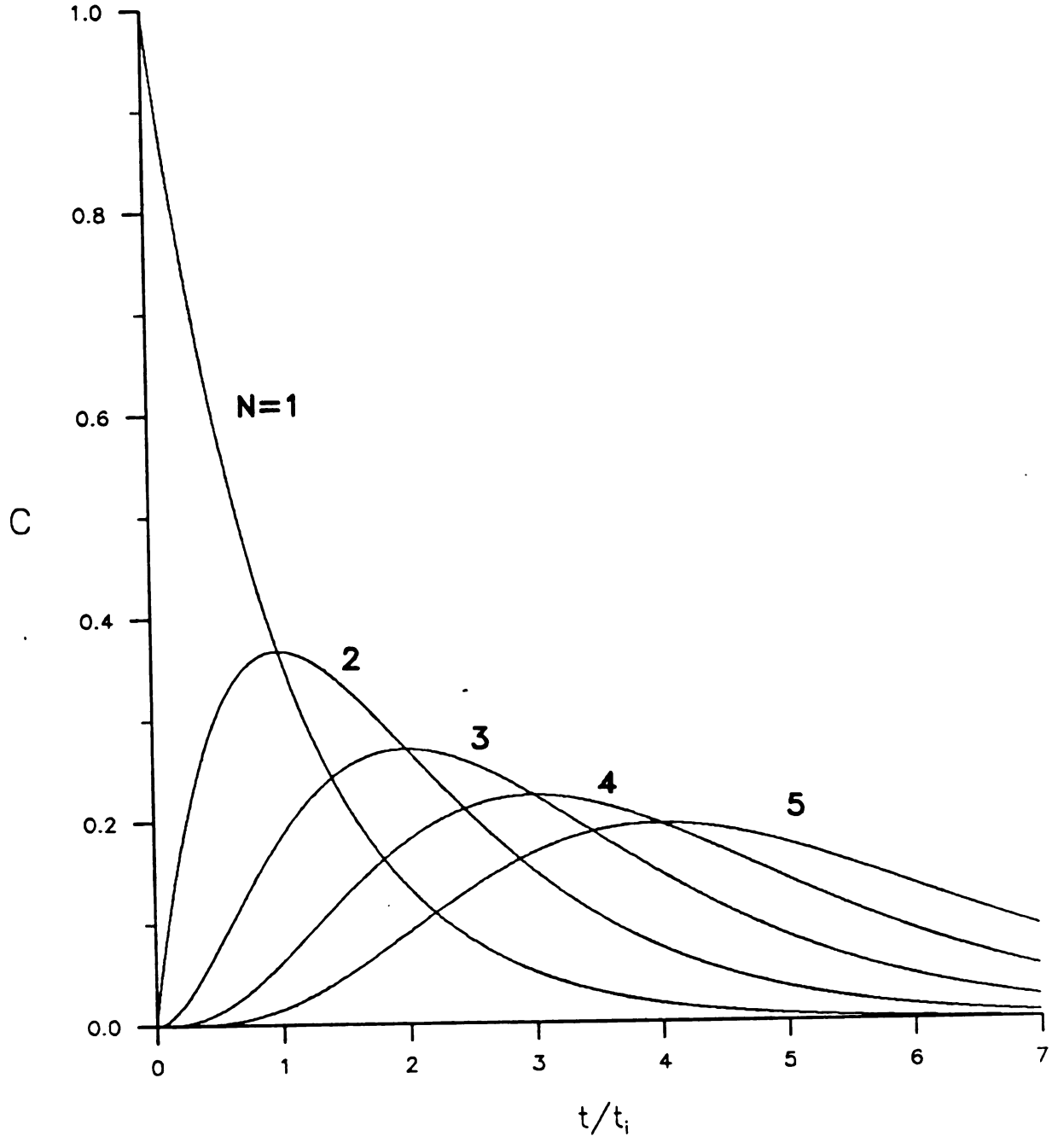

Figure 13. Concentration curves for N=1-5 tanks in series.

const". Under conditions where the Lambert-Beer law is obeyed const'=const". Describing dispersion in this manner reveals the extent to which the sample has been mixed with the reagent in the carrier stream. For D'=1 there is no mixing since $C_o^o=C^{max}$ whereas for D'=2 the sample has been diluted 1:1 with the reagent. With the parameter D', the three classifications of dispersion can be more fully described; for limited dispersion D'=1-3, medium dispersion D'=3-10, and for large dispersion D'>10 [2].

Another manner in which dispersion can be controlled is through the sample volume. When only one mixing stage is used, the rising and falling parts of the C-curve are both exponential and the reverse of each other. The rising curve is

$$C=C_o^o(1-e^{-ks}) \tag{12}$$

and the falling curve is

$$C=C_o^o e^{-ks} \tag{13}$$

and therefore

$$S_{1/2}=0.692/k \tag{14}$$

where $S_{1/2}$ is the sample volume necessary to reach 50% of the steady-state value where $C=0.5C_o^o$ corresponding to D=2. Injecting two $S_{1/2}$ volumes enables 75% of C_o^o to be reached, which corresponds to D=1.33. The injection of seven $S_{1/2}$ volumes yields D=1.008 where $C=0.992C_o^o$. Therefore D=1 cannot actually be reached [2]. Since the steady-state concept is not used in FIA, the maximum sample volume is generally on the order of two $S_{1/2}$ volumes or less for limited dispersion. Injecting a volume corresponding to a fraction of $S_{1/2}$ is a convenient way to dilute a concentrated sample which would have otherwise required predilution.

The value for $S_{1/2}$ depends on the diameter of the manifold, since the same sample volume occupies a larger length in a smaller diameter tube. The volume a sample occupies in a tube is

$$S_v = \pi r^2 l_s. \tag{15}$$

If the tube diameter is halved, the sample occupies a fourfold longer length. This results in a smaller degree of mixing and dispersion. It is for this reason that the tube diameter should be kept small if low or medium dispersion is required. With narrow tubes the reagent consumption is also less since the pumping rate in a tube of radius r is one-fourth that required for a tube of radius 2r to obtain the same linear flow velocity. The use of too narrow tube diameter should be avoided since the flow resistance increase could prevent the use of a peristaltic pump, and the manifold can be easily plugged by small particles unless the solutions are filtered prior to use. Therefore, injecting a minimum sample volume of one $S_{1/2}$ into a manifold of small diameter with the shortest possible line between the injector and the detector is the best way to obtain limited dispersion. The effect of sample volume on the concentration profile is shown in Figure 14.

Up to this point dispersion has been described in terms of peak height. Under the conditions that all other parameters, such as sample volume, concentration of reagents, pumping rate, and all instrument settings remain constant, the areas under the peaks are identical if the flow-through detector is placed at various distances downstream. This is because no color, in colorimetric determinations, is lost or formed during dispersion. Using the convention that peak area is equivalent to the peak height H multiplied by the peak width at half peak height W, the curves can be expressed in terms of the line length,

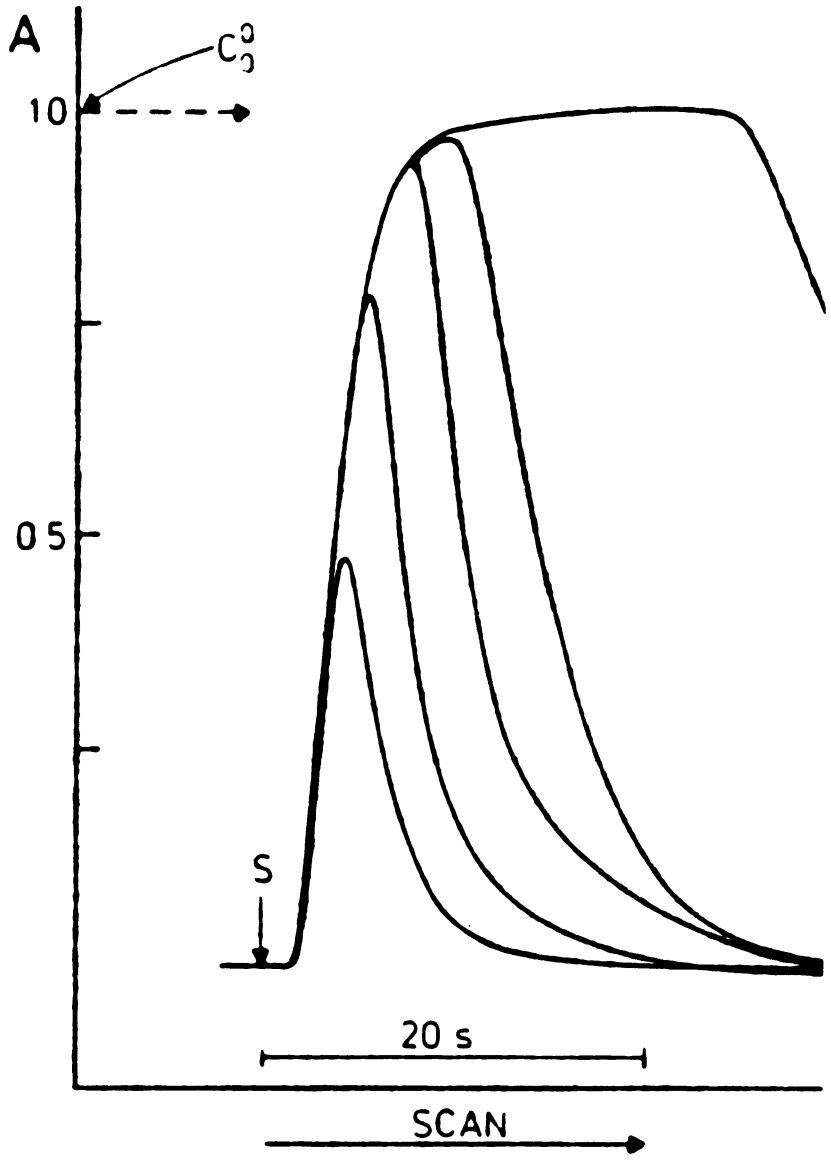

Figure 14. Effect of increasing sample volume on concentration profile.

$$D'=2L^{1/2}1_i^{1/2}/W, \tag{16}$$

the residence time,

$$D'=2QT^{1/2}t_i^{1/2}/W\pi r^2, \tag{17}$$

or the linear flow velocity,

$$D'=2FT^{1/2}t_i^{1/2}/W. \tag{18}$$

From these three equations the generalization can be made that the dispersion of the sample zone varies with the square root of the distance traveled (Equation 16) or the residence time (Equations (17), (18)) and linearly with the flow rate (Equations (17), (18)). Therefore, the desired method for longer residence times with reduced dispersion is to keep the line length short and the flow velocity or pumping rate low. Long residence times, which are difficult to obtain in FIA, can be obtained by intermittent pumping, (stopping the forward movement of the flow stream for a desired incubation period and then resuming pumping). Measuring peak width to determine concentration has been determined by Ruzicka and Hansen [22] to be more subject to experimental errors than peak heights.

If the technique to be used is a gradient technique or one requiring a large dispersion, a mixing chamber can be used to form a well-defined concentration gradient. One example of an application of large dispersion is a flow injection titration. Here the sample zone is well-defined along the time coordinate since it is the peak width that is measured and not the height. The effect of the mixer on the concentration profile can be seen in Figure 15. The mixer greatly reduces the peak height and also broadens the sample width significantly, which greatly reduces the sampling frequency. This reduced peak height yields a signal which is close to the baseline and

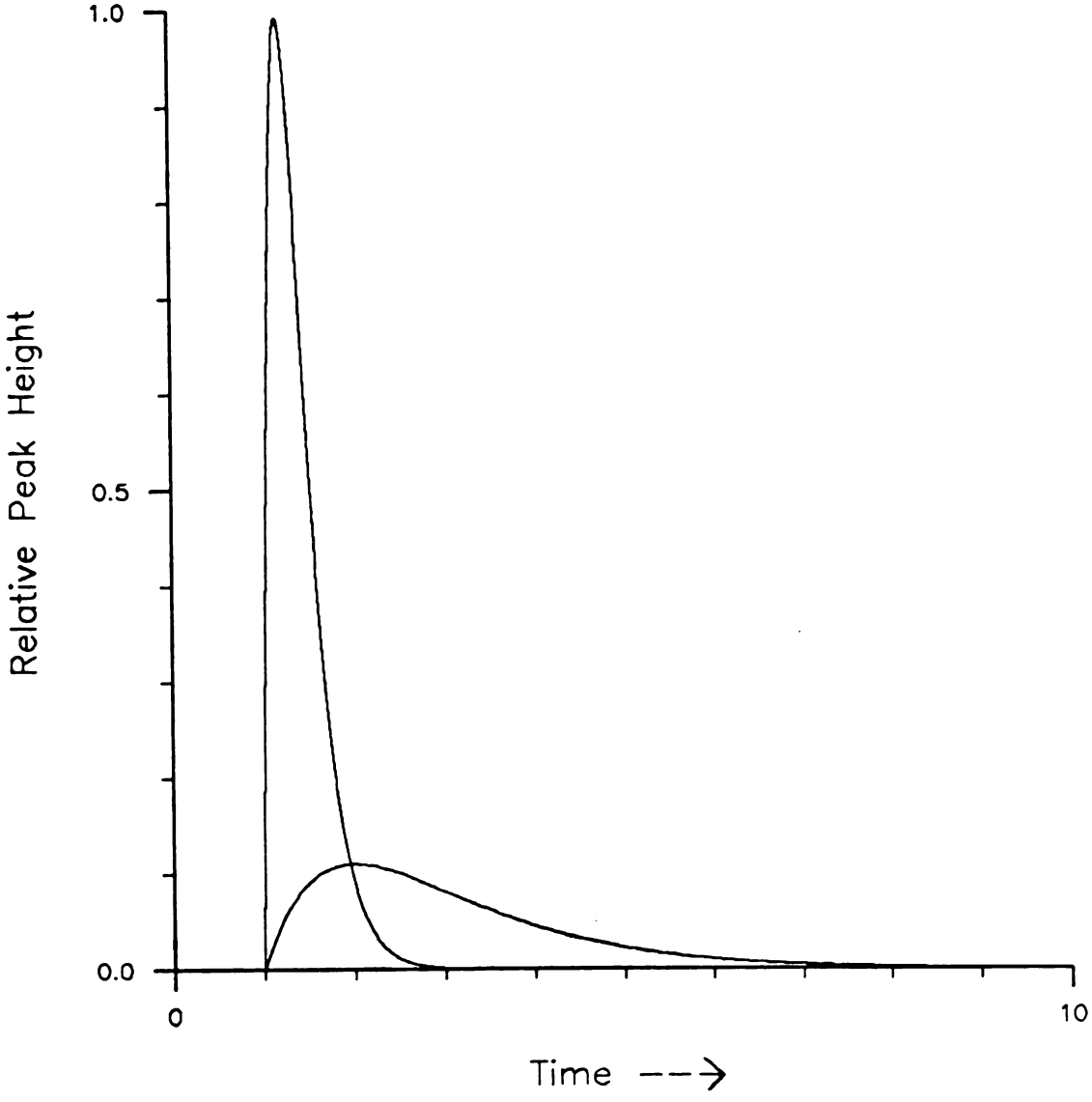

Figure 15. Effect of mixer on concentration profile.

can make integration very difficult if there is an unfavorable signal-to-noise ratio. Consequently, the use of a mixer is a waste of reagent and time and should be avoided if the peak height is the basis of the measurements.

Obtaining limited dispersion in longer manifolds with longer residence times is of interest in FIA. Two methods have been devised to obtain limited dispersion: helically coiled tubing and the single bead string reactor (SBSR). As fluid moves through a helically coiled tube centrifugal forces produce a secondary flow in the radial direction which is perpendicular to the main axial flow [31]. At low flow velocities the centrifugal forces are weak, and the axial velocity profile does not differ much from the profile obtained in straight tubing. At higher flow velocities the secondary flow causes an increase in the radial mass transfer which reduces the axial dispersion. This secondary flow is the result of the formation of two radial circulation patterns which tend to divide the original tube into equal and parallel halves. The axial velocity is the greatest near the center of the tube and it is here that the centrifugal forces act most strongly. Fluid near the center of the tube is replaced by fluid which is being recirculated along the tube wall. Figure 16. shows a cross-section of a coiled tube with a secondary flow pattern. Flow in the coiled tube is characterized by the Dean number Dn,

$$Dn = Re(d_t/d_c)^{1/2} \tag{19}$$

where Re is the Reynolds number (Equations (2), (3)). Coiling the tube tends to stabilize the laminarity of flow. Therefore, the flow rate at which turbulence begins is a much higher value for coiled tubes than for straight tubes.

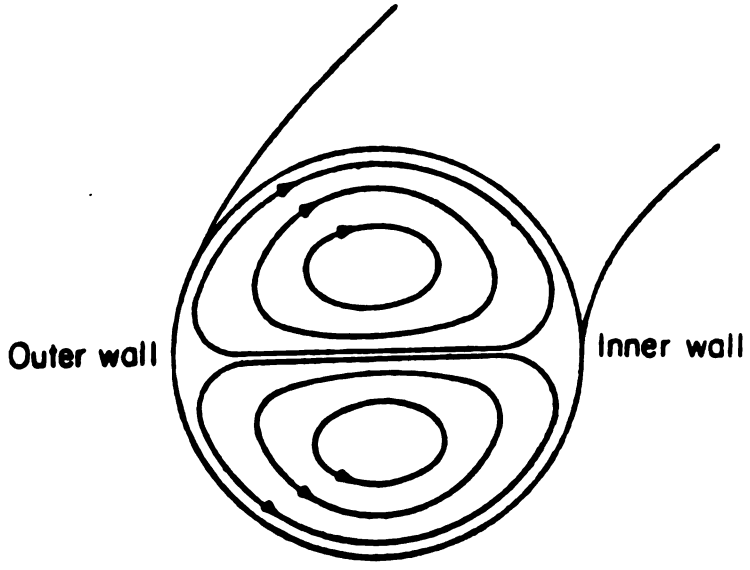

Figure 16. **Cross section of coiled tubing showing secondary flow pattern.**

Knowing that non-uniform velocity distrubutions are a primary cause of dispersion and that radial mass transfer from secondary flow tends to offset the velocity differences, it is apparent that dispersion can be reduced by preventing the parabolic velocity profile from developing and/or by increasing the radial transport. Although the helically coiled tubing does reduce the dispersion somewhat, the SBSR provides a much better reduction in dispersion. Using inert glass beads with a diameter 60-80% of the tubing diameter offers the advantage that no complicated packing techniques are required to obtain a regular zigzag packing pattern. The disadvantage of the SBSR is the high flow resistance which demands a higher pressure capability on the pump, injection valve, and the connections in the Flow Injection system. Figure 17. is an example of the packing pattern in a SBSR. The characteristic concentration profiles for a hypothetical experiment, where a volume of dye is injected into a carrier stream of water, is shown in Figure 18. It is obvious that dispersion cannot be prevented, but the coiled tubing and the SBSR decrease the effect of dispersion and increase the peak height. This reduced disperison also aids in increasing the sampling frequency. Figure 19. represents the comparison of a straight open tube with a SBSR in manifolds of identical residence time, sampling rate, and flow rates. It can be seen that with the SBSR, the dispersion is much less, with baselines being reached between samples; the peak height is also much greater.

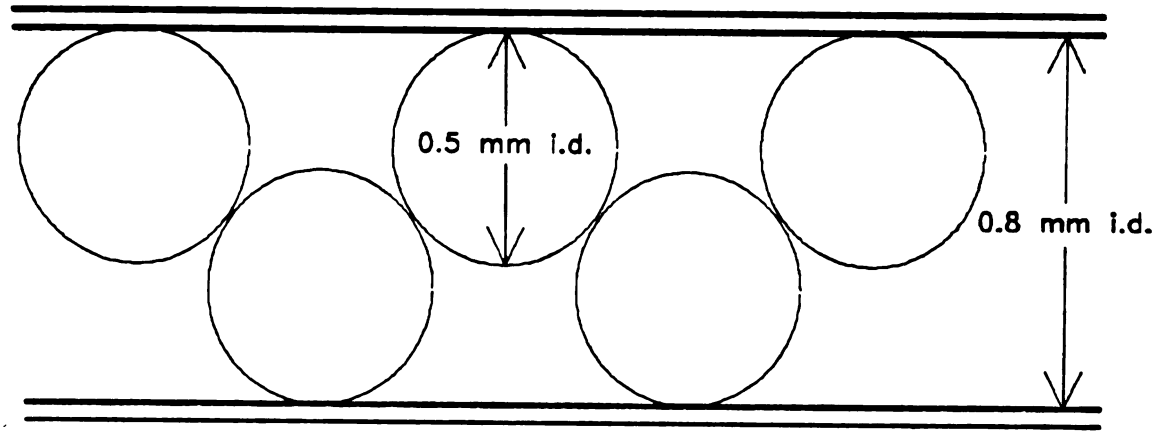

Figure 17. Packing pattern of a SBSR.

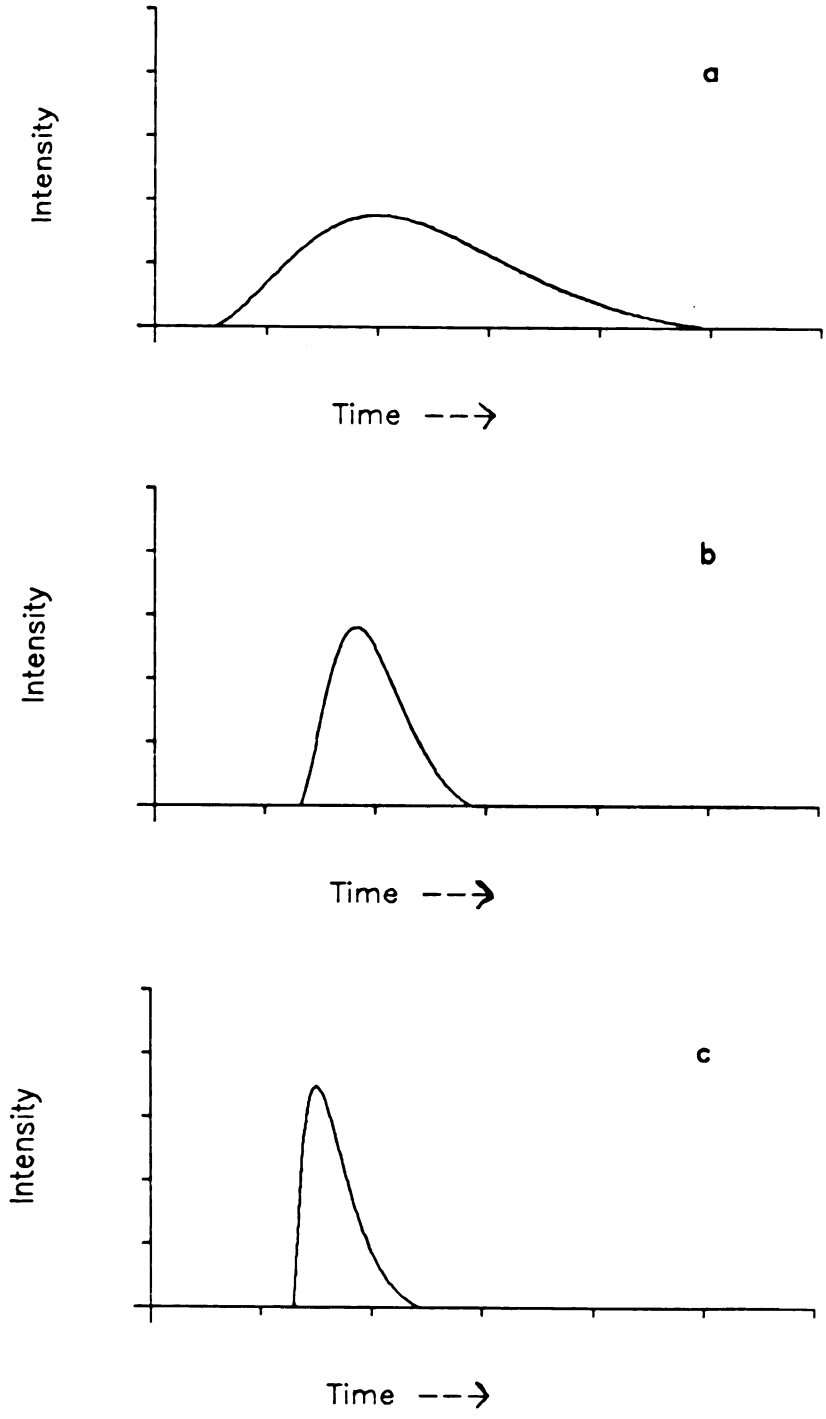

Figure 18. **Comparison of concentration profiles for identical sample volumes injected into a manifold of: (a) straight open tubing, (b) helically coiled tubing, (c) SBSR.**

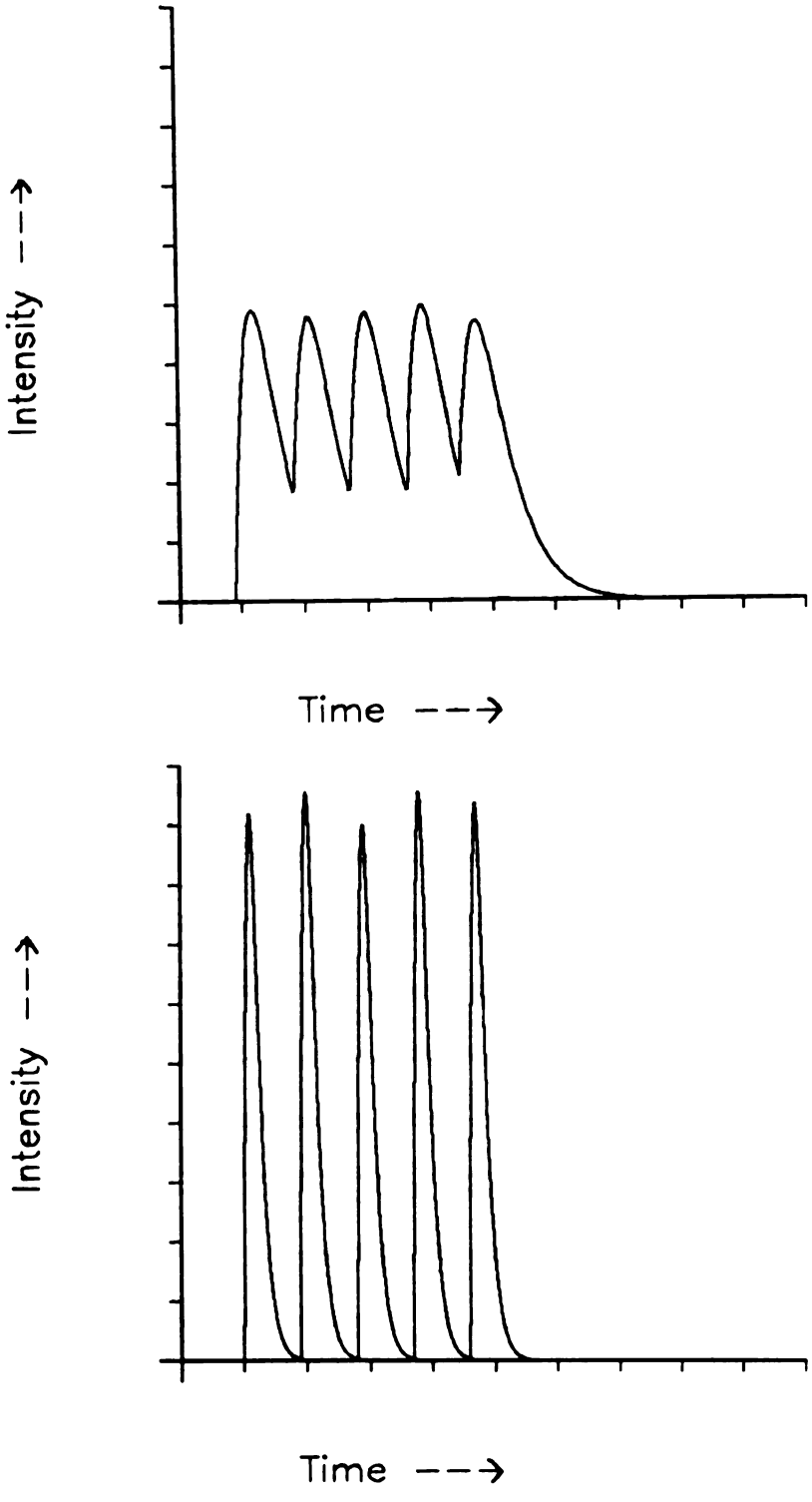

Figure 19. Comparison of straight open tube with SBSR.

REPRODUCIBLE TIMING

Since the steady state signal is usually not measured in FIA, but rather the signal is read off of a steep peak, reproducible timing is critical. This condition is especially true when chemical equilibrium is not reached within the residence time. Reproducible timing is easily obtained in FIA with conventional peristaltic pumps because there are no compressible air bubbles in the flow stream to cause pulsations. By its nature, any stream pulsations in FIA are the result of an imperfect pump.

CFA THEORY

In CFA, air-segmentaion serves to reduce the longitudinal dispersion of the sample along the flow stream. The dispersion in CFA is due to the formation of a thin layer of liquid which wets the inner tube wall. This film follows each segment through the tube and contaminates liquid segments further downstream. Two models have been proposed to explain dispersion in air-segmented flow, the Ideal Model [32] and the Nonideal Model [33]. The ideal model is based on three assumptions: a) there is an instantaneous mixing of the film and the liquid segments which come in contact with it, b) all segments are of constant dimensions and the film has a constant thickness throughout the tube, and c) the longitudinal diffusion in the film is negligibly slow. Figure 20. will be used to illustrate this model of dispersion. The initial sample segment (#0) contains a dye or sample and subsequent segments (#1, #2, etc) are undyed. Segment #0 wets the tube and leaves a film of liquid with a thickness d_f having the same composition as the segment. This film is then mixed into segment #1 due to the flow of

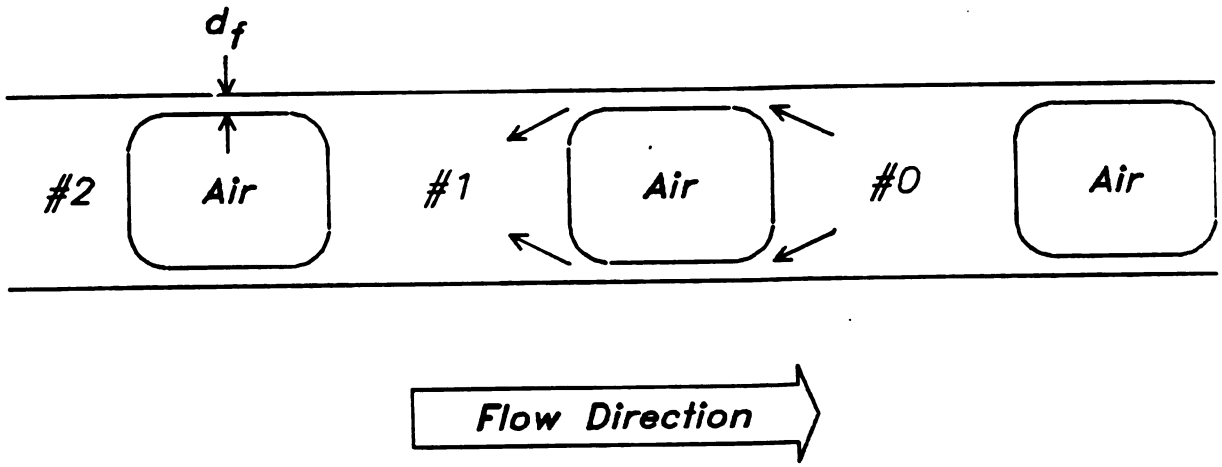

Figure 20. Dispersion in an air-segmented flow stream.

the stream. Segment #2 is then contaminated by #1 in the same fashion. In time, the dye originally in segment #0 is spread throughout several following segments. The concentration of dye in the k^{th} segment can be found from the Poisson distribution function

$$C_k/C=e^{-q}q^k/k! \tag{20}$$

where C is the initial dye concentration in segment #0 and

$$q=V_f/V_s \tag{21}$$

$$q=4d_fL/L_sd_t, \tag{22}$$

where V_f is the volume of liquid coating the interior of the tube from any segment during its passage through a tube length L, and V_s is the volume of a liquid segment of length L_s. A theoretical value for d_f has been related to measurable parameters [34,35].

$$d_f=0.67d_t(v\eta/\gamma)^{2/3}. \tag{23}$$

Combining parameter q from Equation (21) with Equation (23), d_f can be eliminated to yield

$$q=0.67\pi Ld_t^2(v\eta/\gamma)^{2/3}/V_s. \tag{24}$$

With the value of q calculated from measurable parameters the concentration of dye in any segment k can be calculated.

The nonideal model of dispersion takes into account the slow mixing within the moving liquid. The flow pattern of this dispersion is shown diagrammatically in Figure 21. The liquid film deposited by a previous segment will come in contact with the sample bolus at points A and B and is immediately dispersed throughout streamline 1. Mixing then disperses the contaminant into the adjacent streamlines until it is uniformly distributed throughout the segment. From this Bolus Flow pattern it is easy to see that longitudinal mixing across a segment is quite rapid whereas the radial mixing is slow.

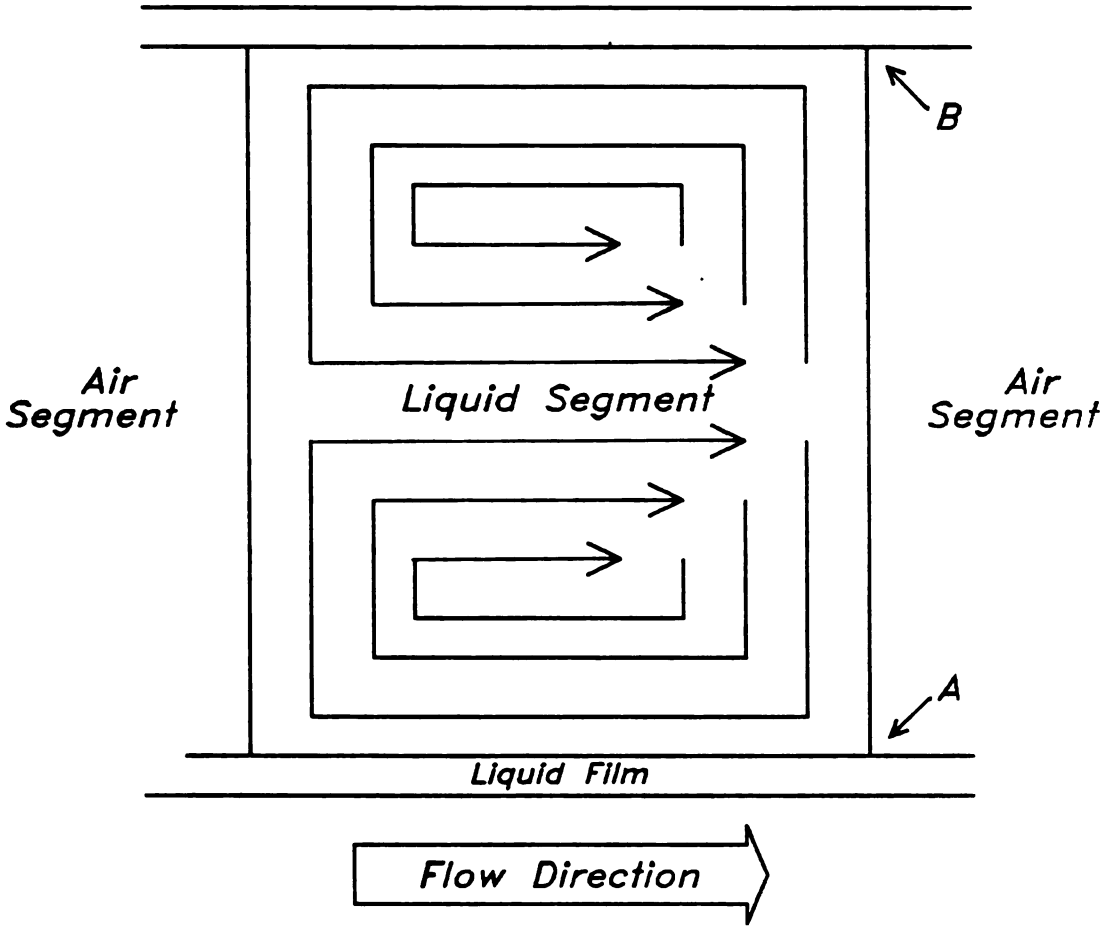

Figure 21. Mixing of liquid segment and liquid film by Bolus flow.

Mixing efficiency is also determined by the liquid's physical properties. Liquid viscosity and density both affect the mixing with viscosity having the most significant effect. Manifold parameters such as internal diameter, helix coil diameter, and segmentation rate also influence the degree of mixing. Short segments mix in less time than long segments, but with short segments a large number of air-liquid interfaces are within the manifold which cause an unacceptable pressure drop across the system. Not only will a large number of small segments increase pulsation as a result of the compressibility of air, but also dispersion increases as the liquid segments become small. Pulsation from peristaltic pumps, which are commonly used in CF systems, results from roller liftoff from the platen. An economical system to minimize the pulsation is to synchronize the injection of an air bubble with the roller liftoff. This type of proportioning has been achieved with an air-bar or a mechanical pinch-valve that opens and closes an air-line in phase with the roller liftoff.

The effect of dispersion on the concentration curve shape in CFA is shown in Figure 22. Just after aspiration of the sample the curve shows a rectangular shape and reaches the baseline during the wash period between samples. The heights of the sample curves are proportional to the analyte concentration in the sample. After dispersion has occured the curves are no longer rectangular in nature, but quite rounded. Figure 22 A. shows the case in which the dispersion is not excessive and a "flat" is still obtained for the sample curve. This "flat" is representative of the nondispersed analyte concentration of the particular sample. The height of the "flat" above the baseline is again proportional to the analyte

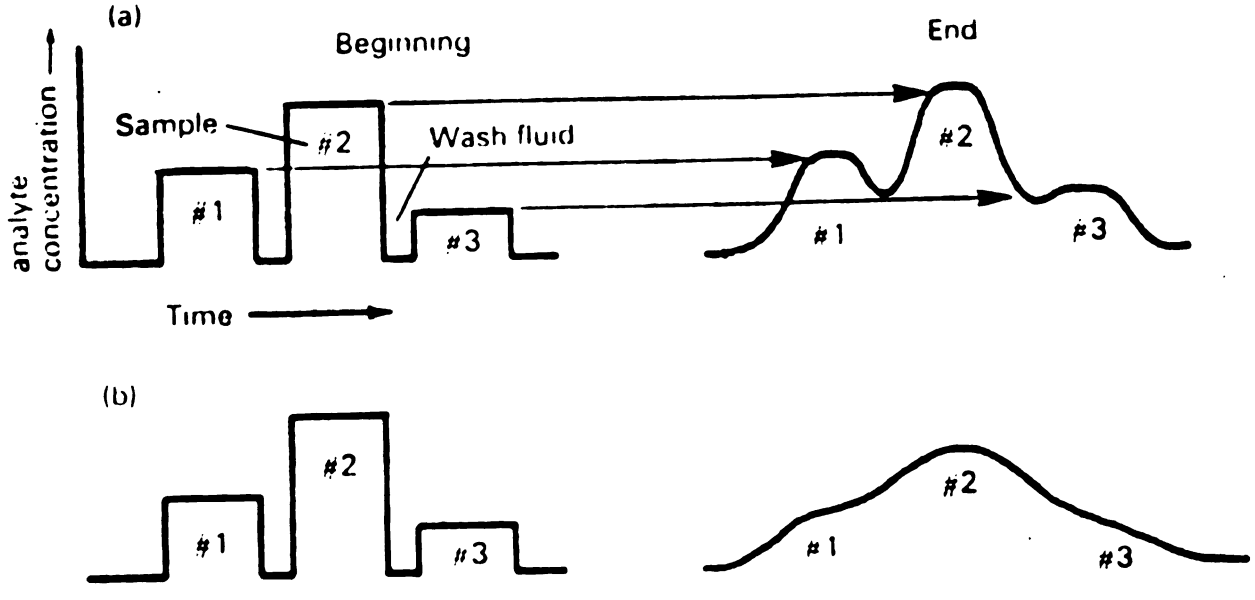

Figure 22. Effect of dispersion in air-segmented analysis. (a) Shows acceptable dispersion whereas the dispersion in (b) is unacceptable.

concentration. Even though the dispersion is minimal in this example, the baseline is not reached between samples.

An unacceptable dispersion can be seen in Figure 22 B. Sample carryover has occurred to the extent that the samples now overlap the "flat" region of the adjacent sample. This has the effect that the apparent concentrations are altered and also that the "flat" time for each sample has been reduced significantly. To avoid this excessive dispersion the intersample wash time can be increased at a cost to the sampling time. This, however, further reduces the "flat" time which results in sample maxima which are not steady-state. The heights of these nonsteady-state peaks are proportional to the analyte concentration and can still be used for the analysis. However, these peak heights are now strongly dependent on the disperison of the system which can change in time. It is for this reason that the use of a nonsteady-state peak should be avoided in CFA.

It is also possible to increase the sampling time to achieve a steady-state peak. This, however, results in lower sample throughput and higher sample and reagent consumption which is also undesirable. Dispersion can be reduced further if the residence time of the sample is kept below 500 seconds [36]. Dispersion in CFA expressed in terms of the variance in time σ_t^2, can now be described in terms of the liquids physical properties, air-segmentation frequency n, and flow rate F [37],

$$\sigma_t^2 = \left[\frac{538 d_t^{2/3}(F + 0.92 d_t^3 n)^{5/3} \eta^{7/3}}{\gamma^{2/3} F D_{w,25}} + 1/n\right]\left[\frac{2.35(F + d_t^3 n)^{5/3} \eta^{2/3} t}{\gamma^{2/3} F d_t^{4/3}}\right] \quad (25)$$

For a particular reaction certain variables are fixed by the requirements of the chemical reaction, η, γ, $D_{w,25}$ and t, the remaining

variables, d_t, F, and n can then be optimized to yield minimum dispersion.

COMPARISON OF FIA AND CFA

Both FIA and CFA are classified as continuous-flow systems and have been used to automate similar chemical analyses [38]. It is desirable therefore to make a comparison of the two techniques. Table I summarizes some basic differences of the two methods. These comparisons are made assuming simple systems.

As a result of the higher sampling rate and shorter start-up and shut-down time FIA may be more suited to relatively rapid analytical methods. However, when long incubation times are required, CFA is the method of choice. Therefore, it appears that there is a place for both FIA and CFA in automated chemical analysis and the choice of one technique over the other depends on the compromises that must be made.

TABLE I

COMPARISON of FIA and CFA

	FIA	CFA
Reagent stream	nonsegmented	gas-segmented
Manifold	simple	more complicated to allow for segmentation
Conduit i.d.	0.3-0.8 mm	1-2 mm
Sample introduction	injection	aspiration
Sampling rate (samples per hour)	150 and higher	typically 60
Sample mixing	controlled dispersion	Bolus flow
Steady state	not required	usually required
Readout time	seconds	minutes
Wash cycle	not required	essential
Reproducibility	better than 1%	better than 1%
Possibility for incubation times longer than 10 min.	not very suitable	suitable
Dialysis/solvent extraction	possible	possible
Titrimetry	possible	not possible
Continuous kinetics analysis	possible with FIA stopped-flow	not possible
Data acquisition	peak height/area or peak width for titrations	recorded peak height
Start-up/shut-down time	seconds	minutes

IV. KINETICS of the LUMINOL-HYPOCHLORITE REACTION

Since 1928 when Albrecht [39] discovered the luminescent properties of luminol (5-amino-2,3-dihydro-1,4-phthalazine-dione) several publications have appeared which have made use of luminol for analytical purposes [40-44]. These publications are partly summarized by Gorus and Schram [45]. To obtain chemiluminescence (CL) from luminol in aqueous solution, an alkaline solution and a strong oxidant are required. For a more efficient reaction, a catalyst or cooxidant can also be included. The quantum efficiency of luminol is quite high with values between 0.01 and 0.05 being reported depending upon the conditions in the solution [46]. As a comparison, the firefly reaction has an efficiency of nearly unity and for nonbiological CL the quantum efficiency of even the brightest reactions rarely exceeds 0.01 [44].

The CL mechanism of luminol oxidation by hypochlorite is not well characterized because of its complexity. Mechanisms for the CL reaction have been proposed [47,48] under different experimental conditions (pH, ionic strength, and method of sample and reagent mixing). The mechanism proposed by Isacsson *et al.* [48] for alkaline solutions is shown in Figure 23. The intensity of the luminescence is strongly pH dependent; as the pH increases there is a corresponding decrease in the flash intensity. It appears any alkaline pH value can be used if it is kept in mind that there is a tradeoff of higher signal-to-noise ratio at lower pH values against improved stability of

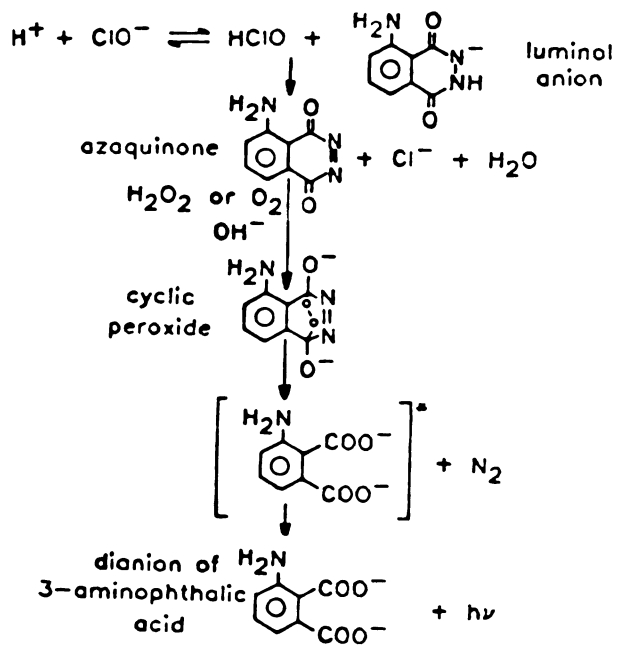

Figure 23. Chemiluminescence mechanism of Luminol-hypochlorite proposed by Isacsson et al. [48].

the CL signal at higher pH values [49].

In the pH range of 9-12 luminol is present as the monovalent anion as shown in the following acidic dissociation constant expressions where H_2L represents the neutral luminol molecule [50]:

$$H_2L \longleftrightarrow H^+ + HL^- \qquad K_1=1.8\times10^{-7} \qquad (I)$$

$$HL^- \longleftrightarrow H^+ + L^{2-} \qquad K_2=6.3\times10^{-13} \qquad (II)$$

The acidic dissociation constant for hydrogen peroxide,

$$H_2O_2 \longleftrightarrow H^+ + HO_2^- \qquad K=2.4\times10^{-12} \qquad (III)$$

has been determined by Joyner [51]. Therefore, in this pH range, H_2O_2 and HO_2^- are present at concentrations high enough to affect the kinetics. The acidic dissociation of hypochlorous acid has been determined by Morris [52]. At 25°C,

$$HOCl \longleftrightarrow H^+ + OCl^- \qquad K=2.95\times10^{-8} \qquad (IV)$$

The value of the equilibrium constant for

$$HOCl + OH^- \longleftrightarrow H_2O + OCl^- \qquad (V)$$

has not been determined, but is estimated to be about $(2\text{-}4)\times10^{10}$ $M^{-1}s^{-1}$ [53]. It has been determined by Balciunas [49] that the peak flash intensity occurs 65-75 ms after the flow-stopped trigger signal was received when a peak-height finding routine was used with a stopped-flow instrument. For any given hypochlorite concentration in that pH range, hydrogen peroxide increases the rate of decay of the flash. This leads to the conclusion that the reacting species which lead to CL are the luminol anion and hypochlorous acid concentrations, which is consistent with the proposed mechanism shown in Figure 23.

FORMATION OF MONOCHLORAMINE

Studies [54,55] of the reactions between hypochorous acid and ammonia in aqueous solutions indicate that the products obtained and their formation rates depend greatly on the pH. Some of the major reactions are as follow [56]:

$$NH_3 + HOCl \longrightarrow H_2NCl + H_2O \qquad (VI)$$

$$NH_3 + 2HOCl \longrightarrow HNCl_2 + 2H_2O \qquad (VII)$$

$$NH_3 + 3HOCl \longrightarrow HCl_3 + 3H_2O \qquad (VIII)$$

Reaction (VII) predominates below pH 4.5 and reaction (VIII) in the pH range of 5.0 to 7.0. Reaction (VI), which predominates above pH 7.5, is the reaction of interest to this study as there is a stoichiometric reaction of ammonia with hypochlorous acid to form monochloramine. Over the pH range of 7.5 to 12.0 the reaction followed second-order kinetics, first-order in ammonia and hypochlorous acid. Second-order rate constants for the formation of monochloramine as a function of pH as determined by Patton [56] are shown in Table II. and graphically in Figure 24. The maximum rate occurs at pH 8.0 which indicates a non-ionic mechanism because the concentrations of ammonia and hypochlorous acid relative to each other are a maximum at this pH.

The rate of monochloramine decomposition decreases as the pH increases. Below pH 10.5 monochloramine decomposition becomes extensive, and above pH 11.5 the rate of monochloramine formation becomes very slow unless there is a very large excess of hypochlorous acid relative to the ammonia concentration [56].

TABLE II

SECOND-ORDER RATE CONSTANT for the FORMATION of MONOCHLORAMINE[a]

pH	C_{init}^{HOCl} (M)	k_{obs} (L mole^{-1} s^{-1})[b]
9.0	1.5×10^{-4}	$2.0 \times 10^{4} \pm 1.2 \times 10^{3}$
9.0	7.4×10^{-4}	$2.1 \times 10^{4} \pm 1.8 \times 10^{3}$
9.0	1.5×10^{-3}	$2.2 \times 10^{4} \pm 1.3 \times 10^{3}$
10.0	1.5×10^{-4}	$6.2 \times 10^{3} \pm 3.1 \times 10^{1}$
10.0	7.4×10^{-4}	$6.1 \times 10^{3} \pm 2.5 \times 10^{1}$
10.0	1.5×10^{-3}	$7.6 \times 10^{3} \pm 5.8 \times 10^{1}$
11.0	1.5×10^{-4}	$7.8 \times 10^{2} \pm 1.6$
11.0	7.4×10^{-4}	$7.9 \times 10^{2} \pm 1.8 \times 10^{1}$
11.0	1.5×10^{-3}	$8.2 \times 10^{2} \pm 2.5$
12.0	1.5×10^{-4}	$7.5 \times 10^{1} \pm 1.9 \times 10^{-1}$
12.0	7.4×10^{-4}	$7.4 \times 10^{1} \pm 1.8 \times 10^{-1}$
12.0	1.5×10^{-3}	$8.0 \times 10^{1} \pm 1.0$

[a] Data from Patton and Crouch, Anal Chem. 49, 464 (1977)
[b] Initial concentration of NH_3 was 1.49×10^{-4} M in all cases

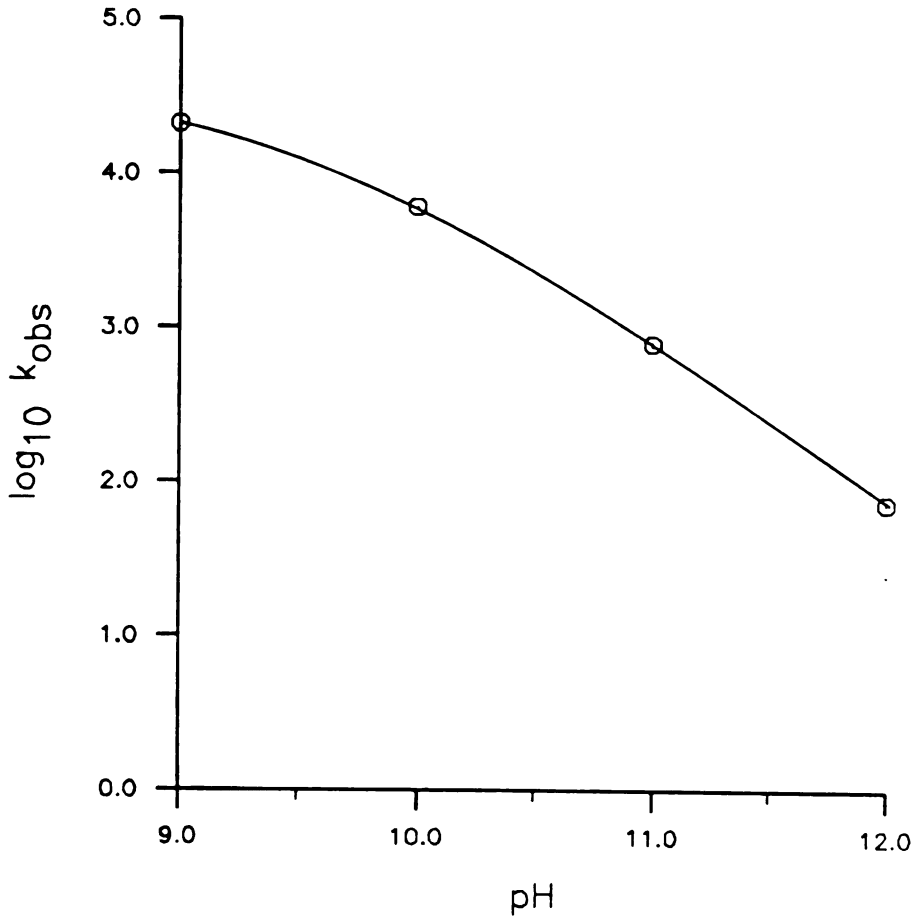

Figure 24. **Log_{10} of observed 2nd order rate constant for the formation of monochloramine vs. pH.**

V. EXPERIMENTAL

A. Equipment and Instrumental

Flow Injection Analysis, with its mechanical simplicity, requires very little equipment. The pump used in all work was a variable speed, twelve channel peristaltic pump (Model IP-12, Brinkmann Instruments, Westbury NY). Flow-rated pump tubes were purchased from Technicon Instruments Corp. (Tarrytown NY). Samples were injected into the carrier stream by a Teflon rotary sample injection valve with a pneumatic actuator (Rheodyne type 50, Anspec Co. Inc., Ann Arbor MI). All manifold conduit was Teflon tubing of either 0.5 mm or 0.8 mm i.d. with 1.5 mm o.d. (Rainin Instrument Co. Inc., Woburn MA).

Since the only source of light is from the chemiluminescence, no monochromator is required. The entire manifold, excluding the pump, was enclosed in a light-proof box. The flow-cell was situated immediately in front of the photomultiplier tube (RCA Radiotron Electron Tube type IP 28). With this arrangement the only source of light striking the PMT is a result of the chemiluminescence. The PMT power supply was a Heath high voltage power supply (Model EU-42A, Heath Corp., Benton Harbor, MI). The PMT output was connected to a current-to-voltage converter (Model 427 current amplifier, Keithley Instruments Inc.) The output signal from the current-to-voltage converter was then either recorded on a strip-chart recorder (Heath

model SR-255 A/B) or acquired by a microcomputer (Intel, 8085 based system) [57]. The microcomputer was programmed in Forth (Forth, Inc.) to perform a twelve bit analog-to-digital conversion on the current-to-voltage converter output [57]. The microcomputer was programmed to remain in a loop acquiring data from the current-to-voltage converter at a frequency of 500 Hz. When the input rises above a pre-determined threshold value the new value is compared against the previous one. This continues until the input value decreases below a pre-determined hysteresis value. At this point the maximum value detected is printed on the terminal screen. The data values were not averaged and if any line fluctuations causing a sudden surge in the input to the microcomputer occurred these values were interpreted as the peak maximum. A zero-crossing switch which only opens or closes the gate when the supply voltge is at zero was used to reduce noise caused by the ac power switch controlling the injection valve actuator.

B. Solutions

All solutions used were prepared in high purity water obtained from a water purification system (Millipore-MilliQ). House distilled water was not used since it was determined that there were sufficient impurities present to inhibit the chemiluminescence reaction [49]. Luminol stock solutions (5 m$\underline{M}$) were prepared from 3-aminophthalhydrazine (#12,307-2 Aldrich Chemical Co. Inc., Milwaukee, WI) in 0.01 $\underline{M}$ KOH without prior purification. Hypochlorite standards were prepared from Clorox which was standardized monthly by the arsenite method [58]. This standardization was required since the

hypochlorite present in the Clorox decomposed; the concentration of hypochlorite had changed from 0.80 M to 0.66 M over a four month period. Luminol and hypchlorite working solutions were prepared in buffers (pH 9.0-12.0) made according to standard methods [59]. Ammonia stock solutions were prepared weekly from reagent-grade ammonium chloride using a method previously reported [56].

Organic buffers (Sigma Chemical Co., St. Louis MO) for the interference studies were prepared in aqueous solutions and used without further purification. Abbreviations for the buffers and their order numbers are: CAPS #C2632, 3-[cyclohexylamino]-1-propanesulfonic acid; creatine #C3630; imidazole #I0125; MES #M8250, 2-[N-morpholino]-ethanesulfonic acid; MOPS #M1254, 3-[N-morpholino]propanesulfonic acid; TAPS #T5130, tris[hydroxymethyl]methylaminopropanesulfonic acid; TES #T1375, N-tris[hydroxymethyl]methyl-2-aminoethanesulfonic acid. All metals for the interference studies were prepared from reagent-grade metal chlorides with the exception of the iron(II) solution which was prepared by dissolving iron wire in a minimum amount of concentrated hydrochloric acid [60].

VI. RESULTS AND DISCUSSION

A. The Flow-Injection Manifold

The manifold used in this study is shown in Figure 25. It was designed to minimize the time that elapses between injection of the sample into the luminol carrier and detection of the emitted light. The rotary injection valve is supplied with leads which are 8 cm long and 0.8 mm i.d. To minimize dead time, the detector lead was changed to a 4 cm, 0.5 mm i.d. Teflon tube. The volume of this length of tubing is ~8µl, which at the 4 ml/min flow-rate employed corresponds to ~120 ms residence time. This narrow diameter lead also serves to minimize mixing prior to detection. This system can then be classified as a limited dispersion manifold.

The flow-cell used is shown in Figure 26. Rule and Seitz [61] have shown that this design is quite efficent as a flow-through luminescence detector. With this type of flow-cell the reaction is observed during mixing or immediately afterwards. This is advantageous for the luminol reaction because the highest intensity is observed at the beginning of the reaction. The first cell designed used a 25 cm Single Bead String Reactor (SBSR) as the coil. The SBSR was constructed from 0.8 mm i.d. Teflon tubing and 0.5 mm o.d. solid glass beads (Propper Mfg., NY). Because the SBSR caused a large back-pressure which caused the injection valve to leak, the SBSR was

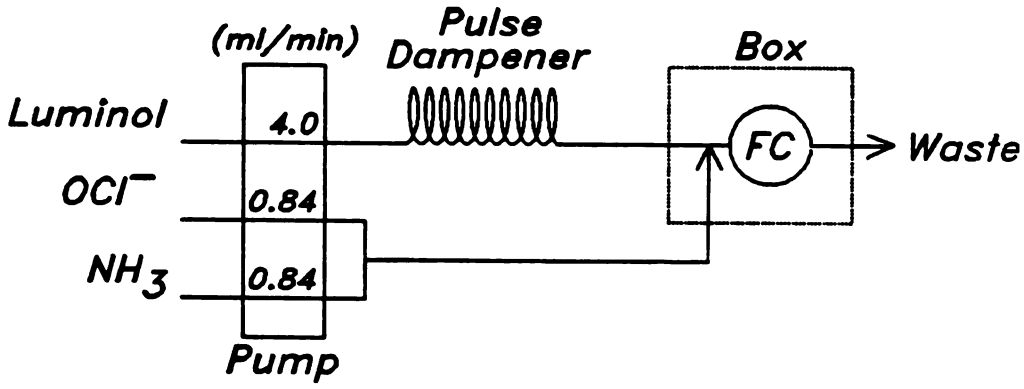

Figure 25. Schematic of flow-injection manifold used for the chemiluminescence determination of ammonia.

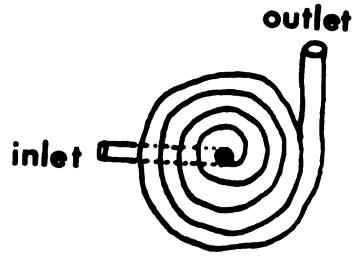

Figure 26. Coiled flow-cell.

later replaced by 25 cm of open 0.5 mm i.d. Teflon tubing. The SBSR was also easily plugged by small particles in the flow-stream.

It was previously mentioned that FIA requires reproducible timing. With the chemiluminescent system employed here, timing reproducibility is highly critical because the luminescence flash occurs very soon after mixing the reagents, and it is desired to make measurements as close to the peak maximum as possible. To minimize the effect of the pump pulsations on the flow rate, a pulse dampener (3 m of 0.5 mm i.d. Teflon tubing) was incorporated into the manifold as shown in Figure 25. In early experiments, pulsations resulting from the rollers lifting off the platen were thought to be minimized by operating the pump at a lower rate. The 4 ml/min flow rate was then achieved by joining two 2 ml/min flow streams in a "T" mixer prior to the pulse dampener. It was later determined that one 2 ml/min flow-rated pump tube operated at twice the nominal flow rate minimized the pulsations to a greater extent. Table III. shows the results of experiments desinged to compare these two manifolds. The rise time (the time taken for the signal to rise from 10% to 90% of full scale) of the current amplifier was varied to determine which value would minimize the noise while maintaining maximum sensitivity. It is obvious from Table III. that the manifold using one pump tube gives better precision with slightly higher peak intensities.

In separate experiments the effectiveness of the pulse dampener was investigated. These results are shown in Table IV. The rise time and the sampling frequency were also varied in these experiments. For rise times of 10 ms and 30 ms there is a significant difference in the standard deviations obtained with and without the pulse dampener.

TABLE III

COMPARISON of MANIFOLD DESIGN and PEAK HEIGHT

Manifold Design	Rise Time (ms)	Average Peak Height[a]
2 tubes	10	3221 ± 108[b]
"	30	3258 ± 154
"	100	3158 ± 87
1 tube	10	3882 ± 14
"	30	3816 ± 25
"	100	3733 ± 80

[a] average of five sample injections
[b] ± 1 standard deviation

TABLE IV

EFFECTIVENESS of PULSE DAMPENER

Rise Time (ms)	Sampling Frequency (inj/min)	Without Dampener Average Peak Height[a]	With Dampener Average Peak Height[a]
10	6	2733 ± 78	2706 ± 44
10	4	2890 ± 42	2784 ± 29
10	3	2731 ± 120	2811 ± 15
30	6	2726 ± 90	2767 ± 24
30	4	2701 ± 85	2776 ± 40
30	3	2768 ± 70	2716 ± 40
100	6	2831 ± 41	2683 ± 30
100	4	2815 ± 40	2681 ± 37
100	3	2747 ± 40	2751 ± 26

[a] averages of five sample injections; ± refers to one standard deviation

There is no significant difference in the standard deviations obtained with the 100 ms rise time. Also the average peak height obtained with the pulse dampener is lower for a 100 ms rise time than for faster values. Thus the 100 ms rise time setting is probably too slow relative to the CL flash to yield accurate results. There is a significant advantage in using the pulse dampener since the the improvement in precision is approximately 50% with the pulse dampener. For all subsequent experiments the rise time was set at 30 ms with a sampling frequency of 6 injections per minute.

The intensity of the signal depends upon the fraction of sample that mixes in the coil in front of the detector. If the length of coil in the flow-cell is increased, more sample is mixed in front of the detector and the CL signal is higher. However, at a certain length the mixing is complete and further increases in the coil length do not lead to further increases in CL intensity. The length of coil is directly related to the volume of sample used; larger sample volumes require longer coils to obtain complete mixing. In order to determine the proper sample volume to obtain complete mixing within the 25 cm coil cell, the manifold shown in Figure 27. was used. A 20 cm mixing coil was used to simulate the leading portion of the flow-cell. With this set-up a 2 µl "Z" cell, shown in Figure 28, was used so that the extent of mixing occurring at the end of the coil cell would be observed. The quartz window exposed to ambient light was covered with black tape to occlude this unwanted light. If the sample volume is too large, the mixing is not complete and a "double peak" is observed. The characteristic double peak is a result of mixing at both ends of the sample zone with the center remaining unreacted. Complete mixing of

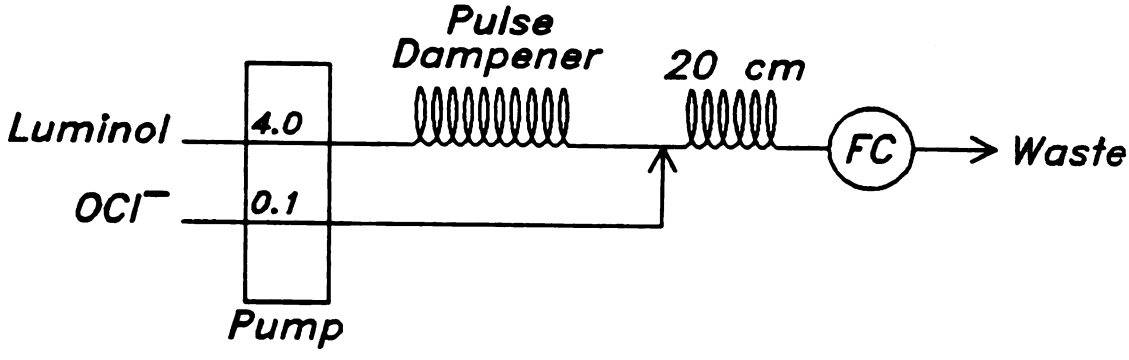

Figure 27. **Manifold used to determine maximum sample volume with complete mixing.**

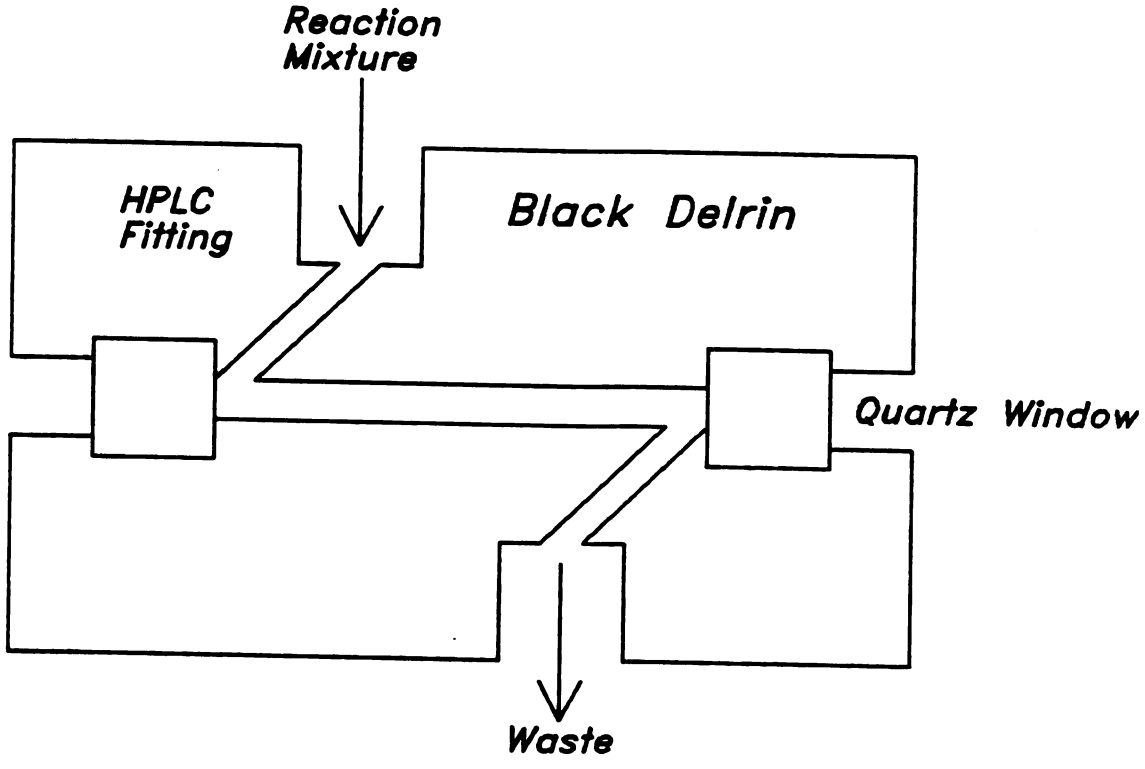

Figure 28. "Z"-Cell.

the sample zone leads to a single peak. Figure 29 shows the peak profiles for sample volumes of 75, 50, and 35 µl. Although the peak height for the 35 µl sample is considerably less than the 75 and 50 µl peaks (the result of a lowered PMT voltage), the peak profiles can still be compared. Both the 75 and 50 µl samples show a considerable double peak. The second peak for the 35 µl sample is a slight shoulder; sample volumes of 25, 10, and 7 µl gave no indication of a second peak. To maximize the sensitivity without obtaining a double peak a sample volume of 30 µl was used for all further experiments.

B. Optimization of Reagents

It was mentioned in the kinetics chapter that the chemiluminescence intensity of luminol is strongly dependent on pH. To investigate this pH dependence, experiments were carried out in various buffer solutions in the region of pH 9.0-12.0. Buffers were prepared from boric acid and potassium hydroxide (pH 9.0-10.5), and from disodium hydrogen phosphate and potassium hydroxide (pH 11.0-12.0). Results of these experiments are given in Table V. and graphically in Figures 30, and 31. The non-linearity of the curves is due to an excess of hypochlorite relative to the 0.65 mM luminol solution. As the pH increases and the flash duration increases, there is a corresponding decrease in the standard deviations of the average peak heights. Above pH 10.0 the average relative standard deviations are 5% or less. However, higher pH's yield lower flash intensities and smaller slopes of the peak-height versus hypochlorite concentration curves. This results in a very poor sensitivity. Consequently, all experiments were carried out at pH 10.5, since the rate of formation of

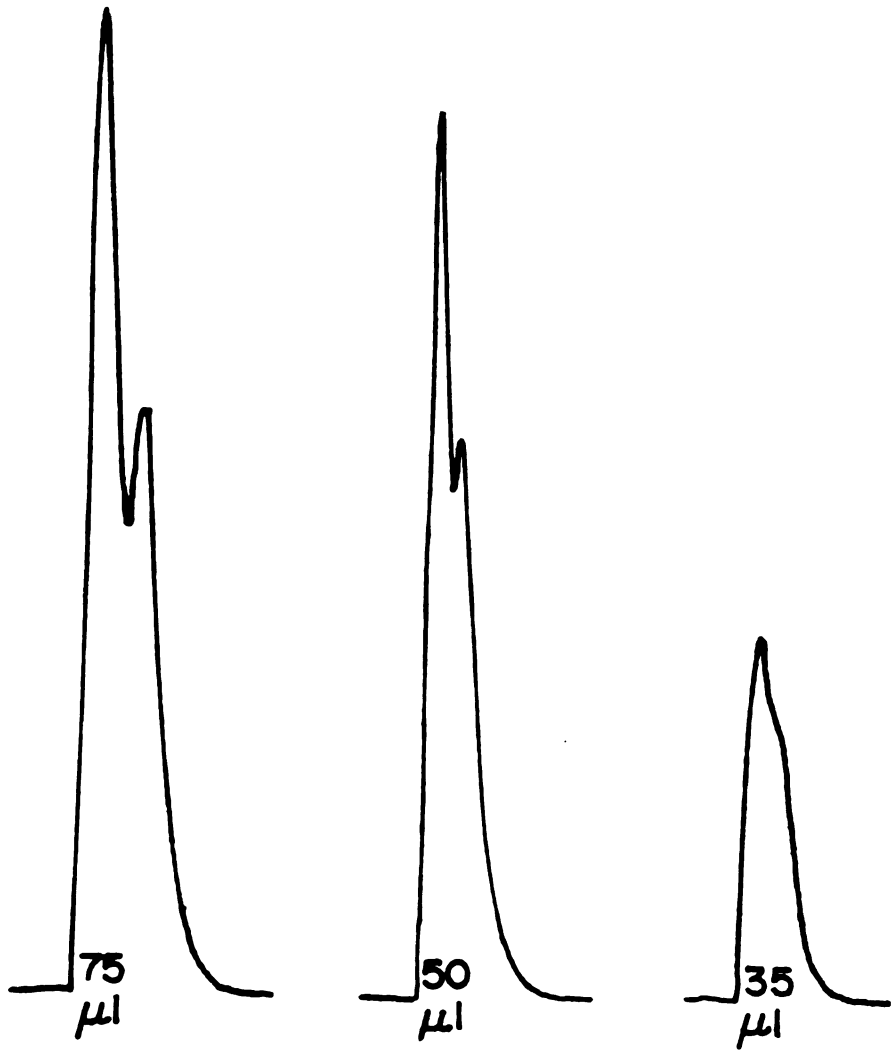

Figure 29. Double peaks resulting from the injection of 75, 50, and 35 µl of sample.

TABLE V

EFFECT of pH on the LUMINOL-HYPOCHLORITE REACTION

$[OCl^-]$ (mM)	PEAK HEIGHT (cm)						
	pH 9.0	pH 9.5	pH 10.0	pH 10.5	pH 11.0	pH 11.5	pH 12.0
0.5	1.13±0.40[a]	2.37±0.35	2.92±0.07	2.20±0.06	0.62±0.02	0.32±0.01	----
1.0	3.47±0.44	4.20±0.18	6.09±0.24	4.26±0.08	1.61±0.03	0.74±0.03	0.29±0.01
3.0	10.38±0.64	10.16±0.94	12.48±0.71	9.03±0.56	4.00±0.13	1.69±0.03	0.74±0.02
5.0	10.94±1.41	14.03±0.85	15.17±0.70	11.45±0.62	5.58±0.35	2.27±0.09	1.09±0.04
7.0	12.16±1.63	13.04±1.36	15.78±1.45	12.38±0.61	5.84±0.43	2.58±0.09	1.31±0.05
10.0	12.98±0.76	14.09±0.61	15.61±1.08	12.57±0.37	7.02±0.45	3.05±0.15	1.60±0.06
Average relative standard deviation (%)	14	8	5	4	5	4	3

[a] average of five sample injections; ± refers to one standard deviation

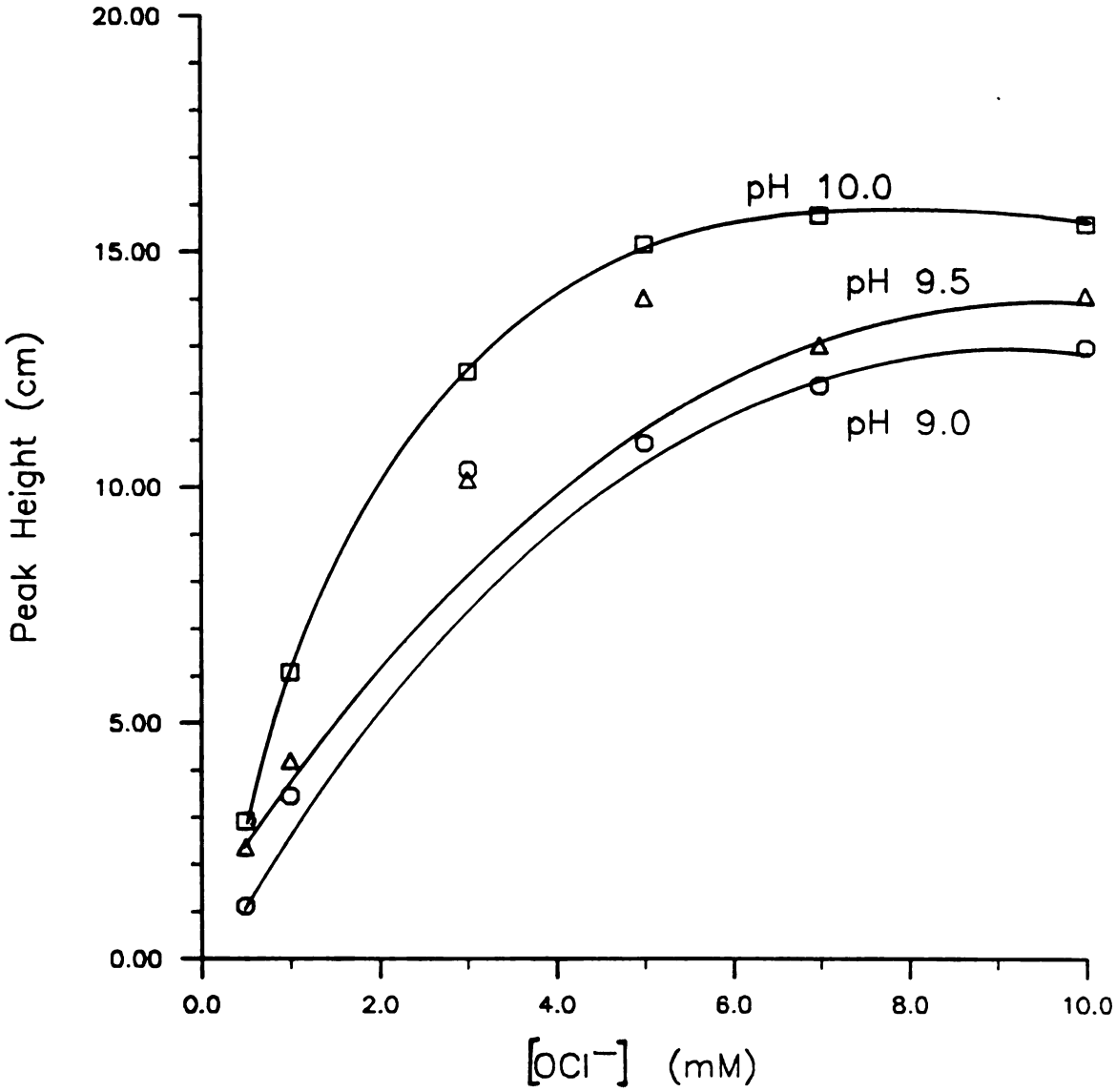

Figure 30. Peak intensity vs. concentration of OCl^- for pH 9.0, 9.5, and 10.0.

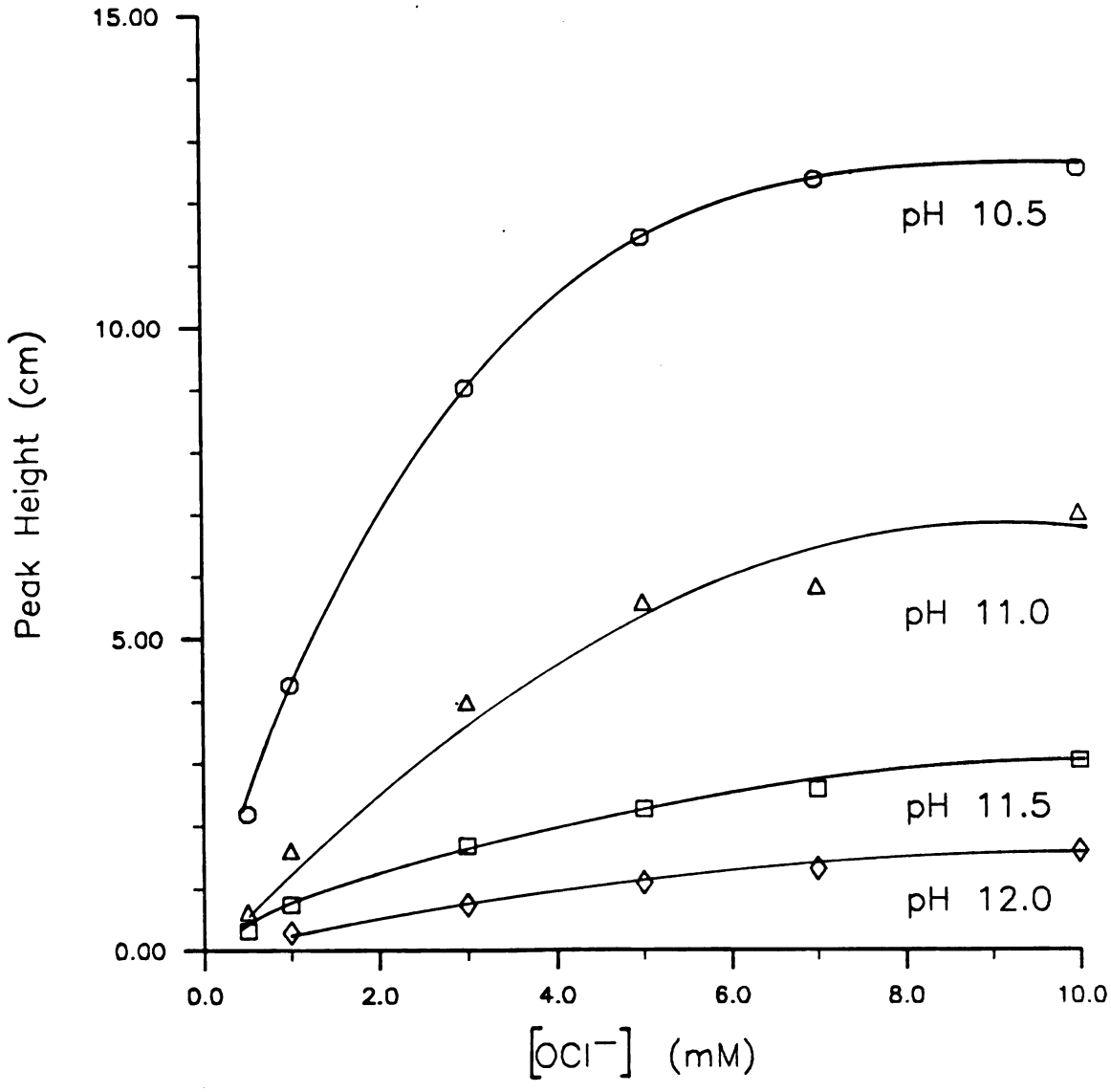

Figure 31. Peak intensity vs. concentration of OCl^- for pH 10.5, 11.0, 11.5, and 12.0.

monochloramine is rapid and stoichiometric at this pH. Monochloramine is also fairly stable with respect to decomposition at this pH [56].

The intensity of the CL signal is strongly dependent on the concentration of luminol. At low luminol concentrations the CL intensity is proportional to the luminol concentration; but at higher concentrations there is non-linear dependence on the concentration of luminol [40]. Marino and Ingle [43] have reported that above 1 mM luminol the CL signal is relatively constant with increasing luminol concentration. For solubility reasons a 2 mM working luminol solution was prepared from a 5 mM stock.

The CL intensity dependence on the concentration of hydrogen peroxide is shown in Figure 32. The observed effect indicates a minimum dependence of the CL intensity on the concentration of hydrogen peroxide at ~2 mM. To minimize the dependence of the CL intensity upon the luminol reagent solution, the concentrations of luminol and hydrogen peroxide were both kept at 2 mM.

The concentration of hypochlorite also influences the observed CL intenstity. This effect is shown is Figure 33. Dilute solutions of hypochlorite were avoided because of their instability. To obtain maximum sensitivity for any given concentration of hypochlorite, a baseline was determined by running water through the sample channel; the PMT voltage was adjusted to yield a peak intensity of 10 volts full scale. To minimize any errors resulting from solution decompositions a baseline correction was performed on all ammonia calibration curves. This correction involves subtracting the peak-height for the ammonia sample from that of the baseline and calculating the corrected standard deviation for the corrected peak-height. With these corrected

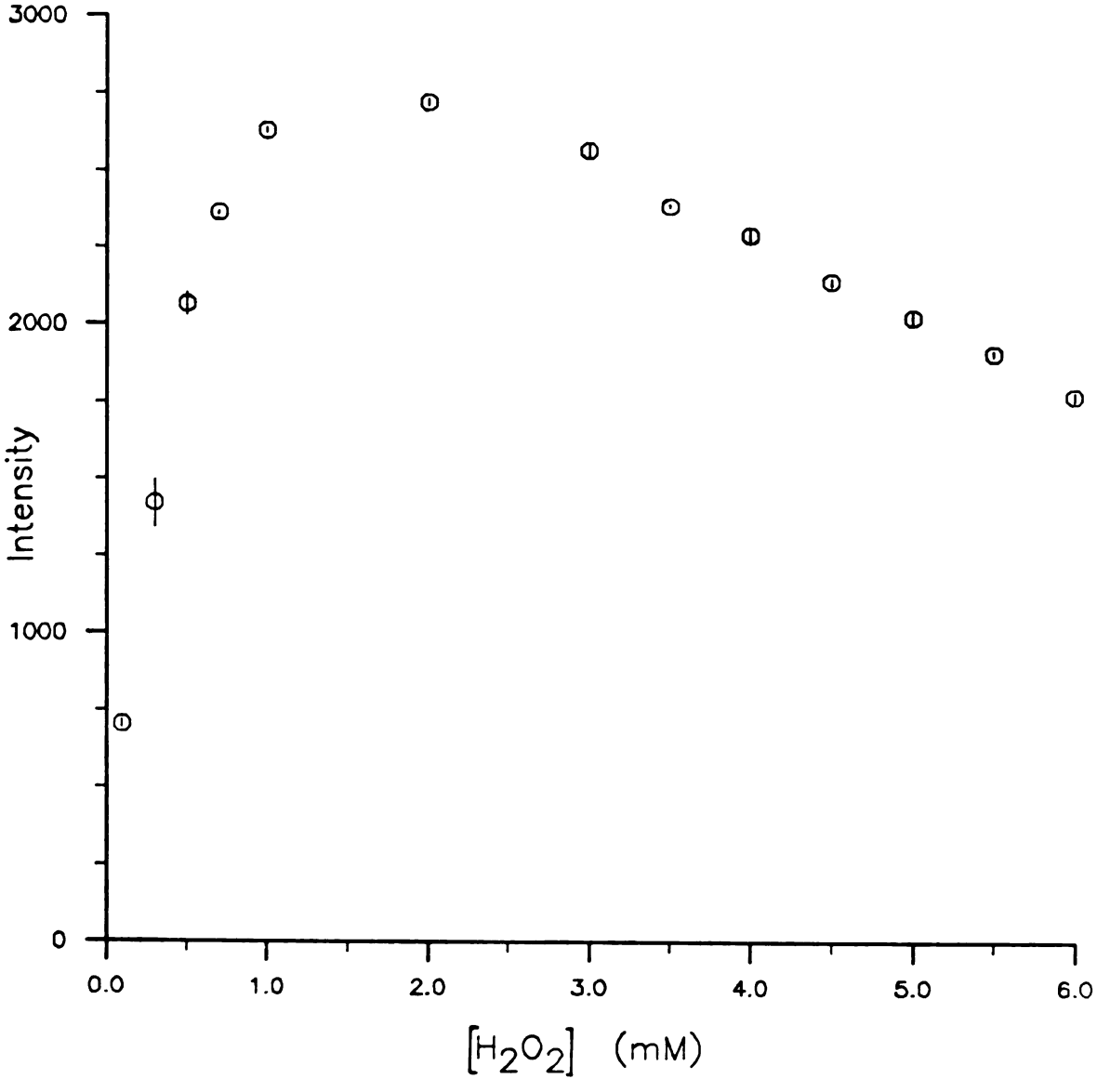

Figure 32. Peak intensity vs. $[H_2O_2]$ with luminol concentration of 2 mM.

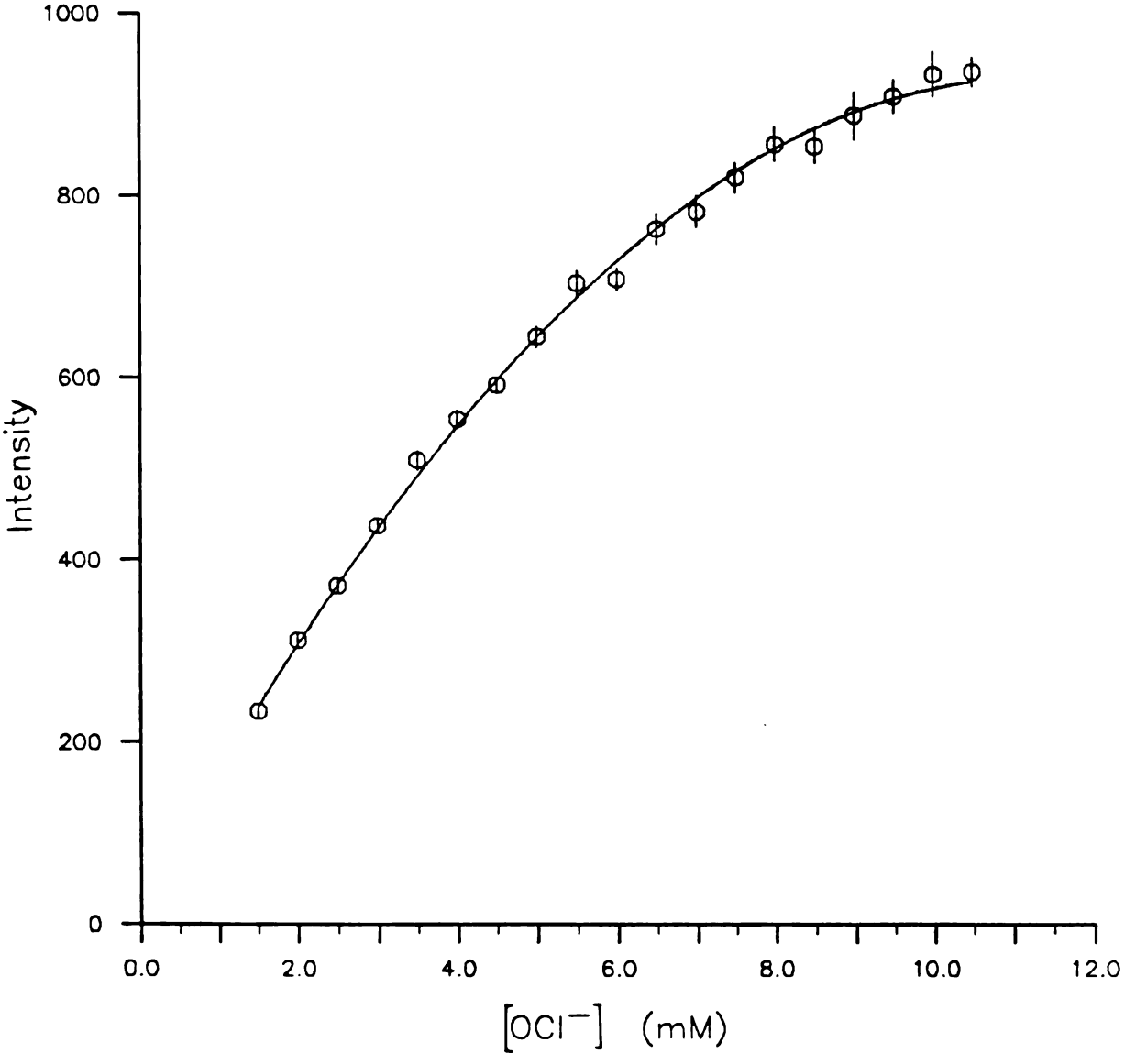

Figure 33. Peak intensity vs. $[OCl^-]$ with luminol and H_2O_2 concentrations equal to 2 mM.

peak-heights the limit of detection of ammonia could be more easily determined. Figure 34. shows calibration curves for ammonia obtained with 2 mM and 5 mM hypochlorite. Although a wider range of ammonia concentrations can be detected with 5mM hypochlorite, a steeper slope and thus higher sensitivity was obtained with 2mM hypochlorite. The data for these two plots are given is Tables VI. and VII. respectively. The limit of detection is defined as that concentration of analyte producing an output signal twice its standard deviation. Thus the detection limits for 2 mM and 5 mM hypochlorite are approximately 0.3 mM and 0.5 mM ammonia respectively. To detect very low concentrations of ammonia the concentration of hypochlorite must be present in at most a ten-fold excess over the ammonia concentration.

C. Interference Study

To determine the usefulness of this system in determinations of ammonia, it is important to investigate the effects of contaminants. This interference study was performed by preparing a 1 mM reference ammonia solution; test solutions were 1 mM in ammonia with the interferent concentration ranging from 1 μM to 100 mM. The concentrations of luminol, hydrogen peroxide, and hypochlorite were 2 mM. Table VIII. shows results for the sixteen interferents tested. The intensity ratio was calculated by

$$\text{Intensity Ratio} = \frac{\text{Peak Height}(NH_3+\text{Interferent})}{\text{Peak Height}(NH_3)}.$$

An intensity ratio greater than unity indicates that the CL signal is enhanced by the interferent while a ratio less than unity indicates CL suppression. A ratio equal to unity indicates that the compound being tested has no effect upon the CL signal. For this study, the compound

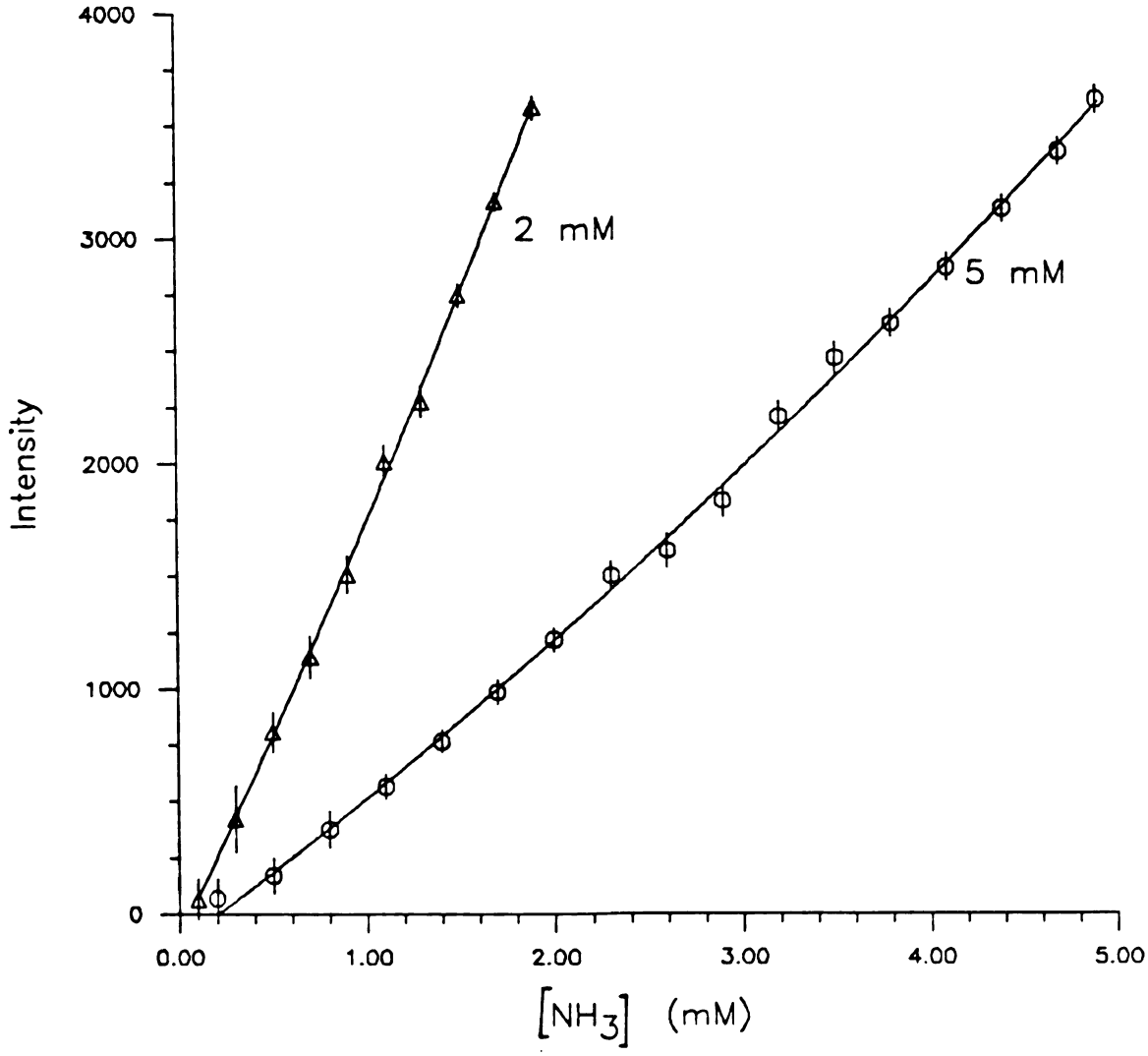

Figure 34. Peak intensity vs. $[NH_3]$ for 2 mM and 5 mM OCl^-.

TABLE VI

AMMONIA CALIBRATION DATA with 2 mM OCl^-

$[NH_3]$ (mM)	Raw Peak Height[a]	Corrected Peak Height[a]
0.00	3774 ± 63	-----
0.10	3709 ± 62	65 ± 88
0.00	3641 ± 49	-----
0.30	3219 ± 85	422 ± 98
0.00	3898 ± 58	-----
0.50	3088 ± 69	809 ± 90
0.00	3869 ± 82	-----
0.70	2726 ± 43	1143 ± 93
0.00	3906 ± 73	-----
0.90	2398 ± 39	1508 ± 83
0.00	3994 ± 64	-----
1.10	1986 ± 38	2007 ± 75
0.00	3898 ± 62	-----
1.30	1620 ± 29	2278 ± 69
0.00	3943 ± 49	-----
1.50	1193 ± 14	2751 ± 51
0.00	3958 ± 39	-----
1.70	789 ± 12	3169 ± 40
0.00	3949 ± 49	-----
1.90	364 ± 13	3585 ± 51

[a] average of five sample injections; ± refers to one standard deviation

TABLE VII

AMMONIA CALIBRATION DATA with 5 mM OCl^-

$[NH_3]$ (mM)	Raw Peak Height[a]	Corrected Peak Height[a]
0.00	3891 ± 63	-----
0.20	3823 ± 58	68 ± 85
0.50	3721 ± 49	170 ± 79
0.00	3938 ± 53	-----
0.80	3563 ± 64	375 ± 83
1.10	3372 ± 10	566 ± 54
0.00	3867 ± 40	-----
1.40	3100 ± 29	767 ± 49
1.70	2882 ± 35	985 ± 53
0.00	3900 ± 46	-----
2.00	2680 ± 25	1219 ± 52
2.30	2398 ± 39	1502 ± 60
0.00	3881 ± 70	-----
2.60	2268 ± 30	1613 ± 76
2.90	2047 ± 13	1834 ± 71
0.00	4011 ± 65	-----
3.20	1802 ± 18	2208 ± 68
3.50	1540 ± 16	2471 ± 67
0.00	3867 ± 60	-----
3.80	1244 ± 6	2623 ± 60
4.10	994 ± 17	2874 ± 62
0.00	3836 ± 60	-----
4.40	701 ± 6	3135 ± 61
4.70	447 ± 8	3389 ± 61
0.00	3878 ± 61	-----
4.90	259 ± 2	3620 ± 61

[a] average of five sample injections; ± refers to one standard deviation

TABLE VIII

EFFECT of INTERFERENTS

Interferent	Intensity Ratio					
	1μM	10μM	100μM	1mM	10mM	100mM
Imidazole	——	1.02	1.01	1.19	1.69	1.44
MOPS	0.99	1.02	1.02	1.10	0	0
MES	———	1.00	1.02	1.04	0.83	0
CAPS	0.99	1.00	0.90	0.03	0	0
Creatine	1.01	1.01	0.99	0.85	0	0
TAPS	0.99	0.97	0.82	0	0	0
TES	1.01	0.97	0.85	0	0	0
Ni^{2+}	1.03	1.01	0.98	1.02	1.27	0.19
Fe^{3+}	0.99	0.99	1.01	1.08	1.68	0.08
Fe^{2+}	1.02	1.01	0.89	0.69	0	0
Cu^{2+}	0.94	0.86	0.91	1.10	>2	>2
Mn^{2+}	1.03	1.01	0.96	0.79	0.84	0.52
Co^{2+}	1.00	0.99	0.96	0.91	0.17	0
NaCl	1.07	1.05	0.98	1.00	0.98	0.99
KCl	1.00	1.02	0.97	0.98	0.98	0.98
$MgCl_2$	0.97	0.98	0.99	1.01	1.03	1.17
Na_2CO_3	0.99	0.99	0.98	1.01	0.87	0.52

of interest was considered to be an interferent if the intensity ratio was greater than 1.1 or less than 0.9; that is, a 10% change in the output signal.

The first compounds tested were organic buffers which are known to interfere with ammonia determinations by the Berthelot method [62]. Three mechanisms for the interference have been postulated. These buffers all possess amine groups which have been found to follow second order kinetics in the formation of alkylchloramine [54],

$$RR'NH + HOCl \longrightarrow RR'NCl + H_2O \qquad (IX)$$

The rates of formation of these alkylchloramines vary with pH in the same manner as the formation of NH_2Cl [54]. With the exception of imidazole, all the compounds in this group exhibit a suppressive effect on the CL signal.

Several of these compounds, creatine, MES, MOPS, TAPS, and TES, are acidic ($pK_a \leq 8$) relative to the working pH 10.5. It is possible that the acidity of these compounds, when present in sufficient concentrations, is high enough to cause the pH to shift to a lower value. It was mentioned earlier that at lower pH's the CL flash occurs earlier in time. If the flash occurs too early to be fully detected, the observed peak-heights would be low.

The third mechanism of interference involves the amine group of the interferent combining with the azoquinone intermediate of the luminol-hypochlorite CL reaction (see Figure 35.). Quinones are susceptible to nucleophilic attack by amines or other necleophiles [63]. It is possible that the amine group on the buffer oxidizes the azoquinone so that the activated species leading to CL is not formed. This again would result in a suppresion of the CL signal.

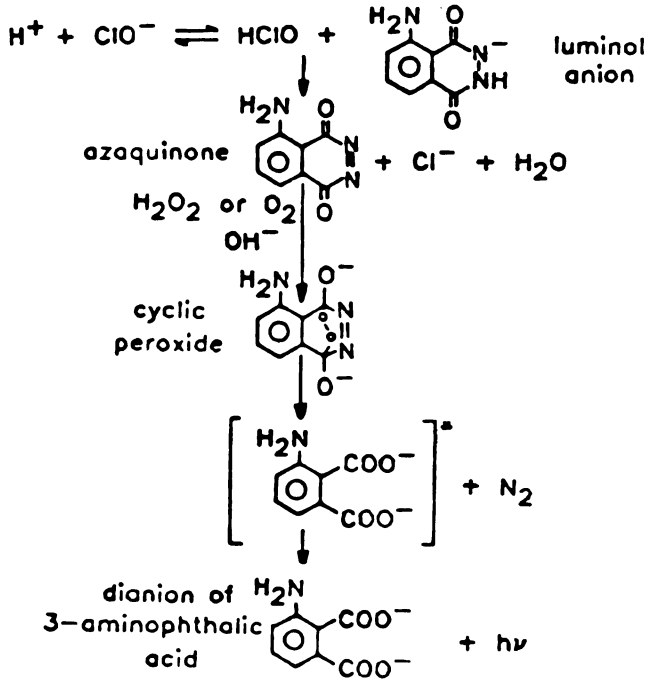

Figure 35. Chemiluminescence mechanism of luminol-hypochlorite proposed by Isacsson et al. [48].

The second class of compounds tested for interference consisted of transition metal cations: Ni^{2+}, Fe^{3+}, Fe^{2+}, Cu^{2+}, Mn^{2+}, and Co^{2+}. These metal ions are known to catalyze the luminol reaction in the presence of peroxide [64] and show an interference effect at concentrations greater than 10 mM (a ten-fold excess over ammonia).

Several compounds which should not interfere with the luminol-hypochlorite reaction were also tested: KCl, NaCl, $MgCl_2$, and Na_2CO_3. As shown in Table VIII, Na_2CO_3 supresses the CL signal when present in ten-fold excess over the ammonia. This is thought to be a pH effect. The CL signal is increased slightly by $MgCl_2$ when present in a one hundred-fold excess.

Anomalous results were obtained for imidazole, Fe^{3+}, and Ni^{2+}. The results are shown graphically in Figure 36. No explanation for their behavior could be found. Out of the sixteen samples tested, only two, KCl and NaCl, were found not to interfere when present in a one hundred-fold excess. This tends to indicate that the luminol-hypochlorite method for ammonia determination is very susceptible to interferents. This is supported by J. D. Ingle [65] who has stated that everything from Ritz crackers to the kitchen sink interferes with CL.

D. Determination of Ammonia in River Water

To test the applicability of the proposed method for ammonia analysis water was obtained from the Red Cedar River and analyzed for ammonia. In order to minimize the effect of interferents upon the CL signal a six inch dialyzer with a 1.0 μm pore size Gore-Tex membrane was used (W. L. Gore and Associates, Inc., Elkton MD). This membrane

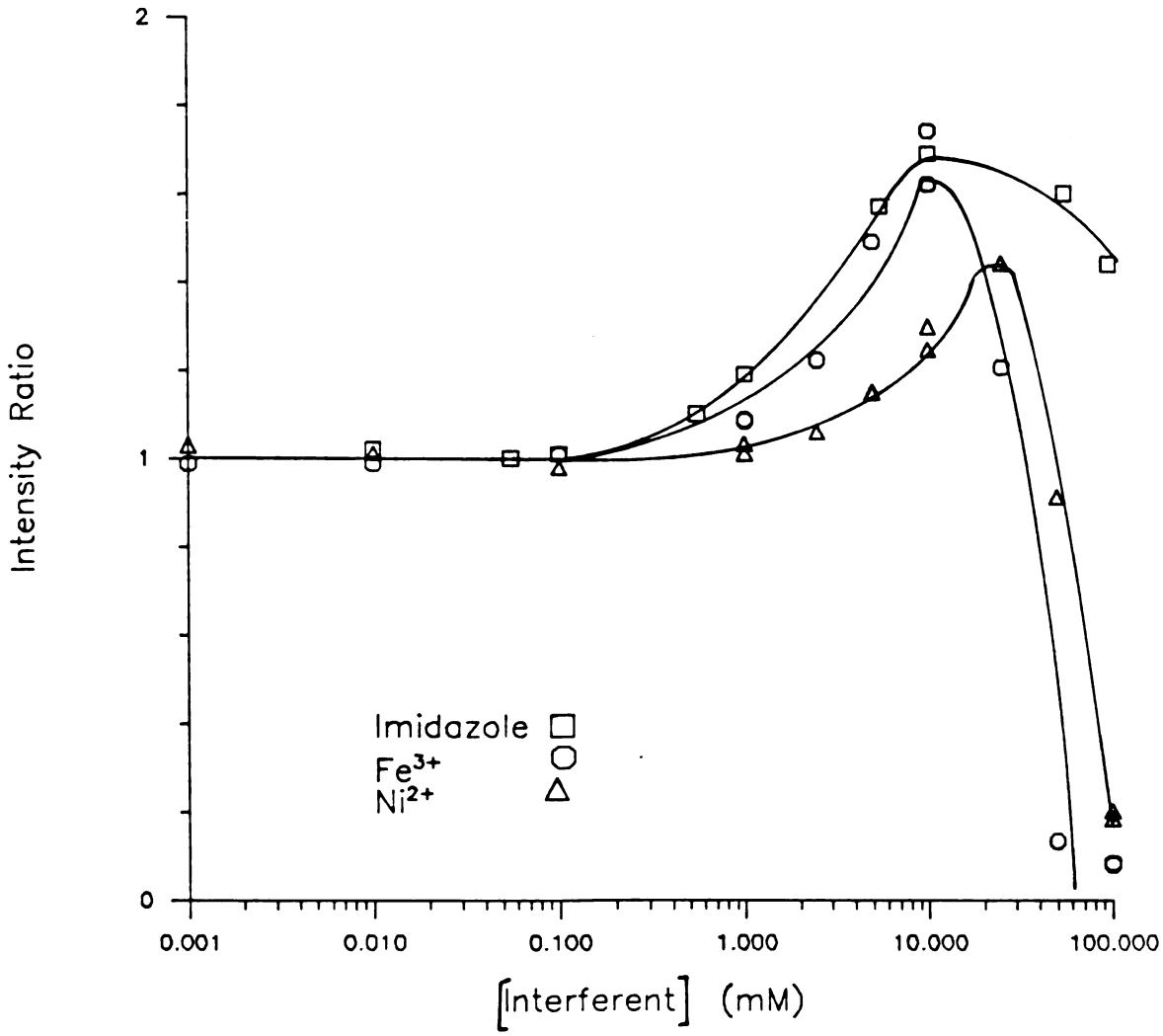

Figure 36. Effect of concentrations of interferents imidazole, Fe^{3+}, and Ni^{2+} on the intensity ratio.

is used as a liquid degasser. The manifold used for this study is shown in Figure 37. The ammonia in the test solution is converted to NH_3 by mixing it with 0.5 M KOH. Ammonia vapor then diffuses across the membrane. To prevent an equilibrium condition from occurring, the recipient stream was MQ water with pH ~6. This slightly acidic recipient stream converts NH_3 to NH_4^+ which will not diffuse through the membrane. The 40 cm SBSR was used to create a back pressure on the donor side of the dialyzer so that the NH_3 would more easily pass through the membrane. In order to obtain a residence time in the dialyzer long enough to pass a detectable amount of ammonia across the membrane the flow-rates through the dialyzer were reduced to the bare minimum. This condition is far from ideal for FIA. The MQ water containing the NH_4^+ was then mixed with hypochlorite to form monochloramine. The concentration of hypochlorite was reduced to 7 μM to obtain maximum sensitivity. Standardization was achieved by determining the CL intensity of 1, 3, 5, and 7 μM ammonium chloride standards prepared in MQ water. Results of this standardization are given in Table IX and Figure 38. The line in Figure 38. was determined by a weighted linear regression on the corrected peak heights to be

$$y = -40 + 65(x). \qquad (27)$$

Solving equation (27) for concentration (x) with a sample peak height (y) of 229 yields a sample concentration of 4 μM ± 1.

To serve as a comparison for the proposed technique, the ammonia was also determined on a Technicon AutoAnalyzer II by the Technicon Industrial Method No. 334-74W/B. This method, designed for the determination of nitrogen and phosphorous in acid digests, is based

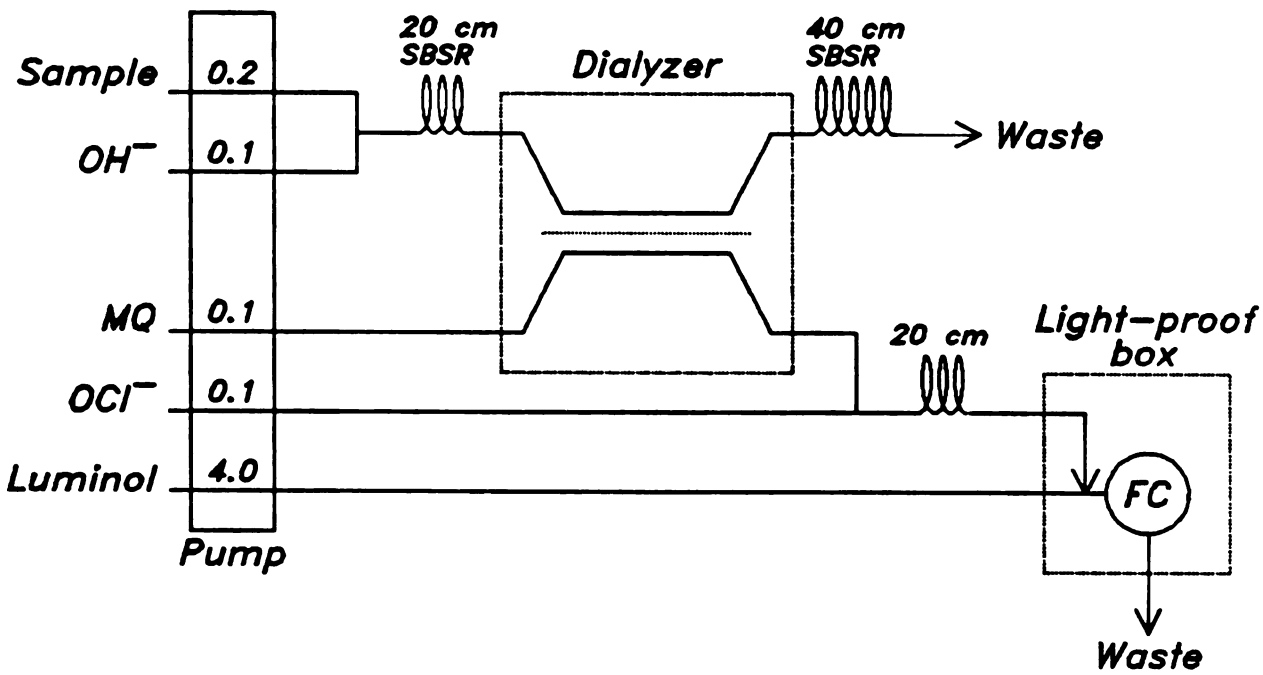

Figure 37. Schematic of manifold used in the determination of ammonia in river water.

TABLE IX

STANDARDIZATION DATA for AMMONIA DETERMINATION (FIA)

$[NH_3]$ (μM)	Raw Peak Height[a]	Corrected Peak Height[a]
0.00	3590 ± 47	———
1.00	3547 ± 21	43 ± 51
3.00	3484 ± 28	106 ± 54
0.00	3543 ± 52	———
sample	3314 ± 39	229 ± 65
5.00	3217 ± 32	327 ± 61
7.00	3144 ± 48	400 ± 71

[a] average of five sample injections; ± refers to one standard deviation

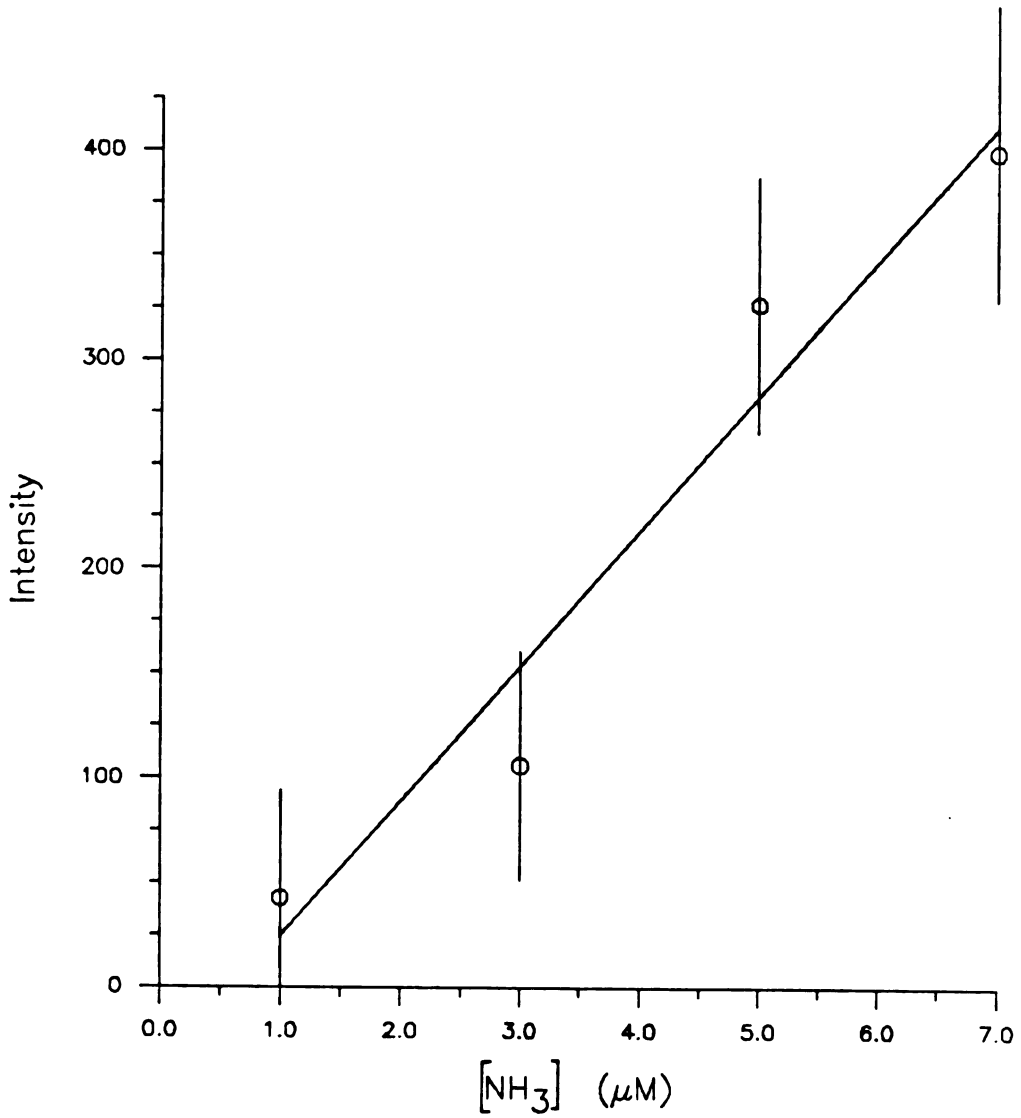

Figure 38. **Calibration curve of peak intensity vs. concentration of ammonia for determination of ammonia in river water by FIA.**

upon the reaction of ammonia, sodium salicylate, sodium nitroprusside, and hypochlorite in a pH 12.8-13.0 buffer. This method uses a substituted phenol (sodium salicylate) in the Berthelot reaction. The generalized reaction mechanism is given in Figure 39. [66]. The absorbance maximum of the ammonia-salicylate is at 660 nm. The concentration of ammonia was quite low and maximum amplification of the colorimeter output was required. Standards of 0, 1, 3, 5, 7, and 9 μM in ammonia were used for standardization. Results for this determination are given in Table X. and Figure 40. The equation for the line in Figure 40 is

$$y = 6.379 + 0.510(x) + 0.0819(x^2). \qquad (28)$$

The average sample height is 7.3 cm corresponding to a concentration of 1.5 μM ammonia.

When it is taken into consideration that the concentration of ammonia detected in these two experiments is not in an optimum detection range, the two results for the concentration of ammonia in the river water compare quite favorably.

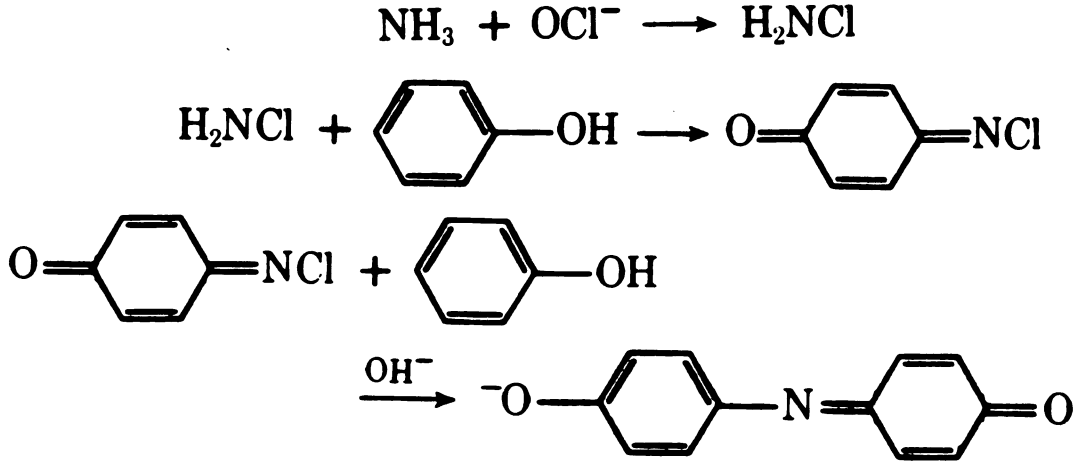

Figure 39. **Generalized mechanism for the Berthelot reaction proposed by Bolleter *et al*. [66].**

TABLE X

STANDARDIZATION DATA for AMMONIA DETERMINATION (CFA)

$[NH_3]$ (μM)	Peak Height (cm)
0.0	6.2
1.0	7.0
3.0	9.1
5.0	11.0
7.0	13.4
9.0	17.9
sample	7.6
sample	7.3
sample	7.0

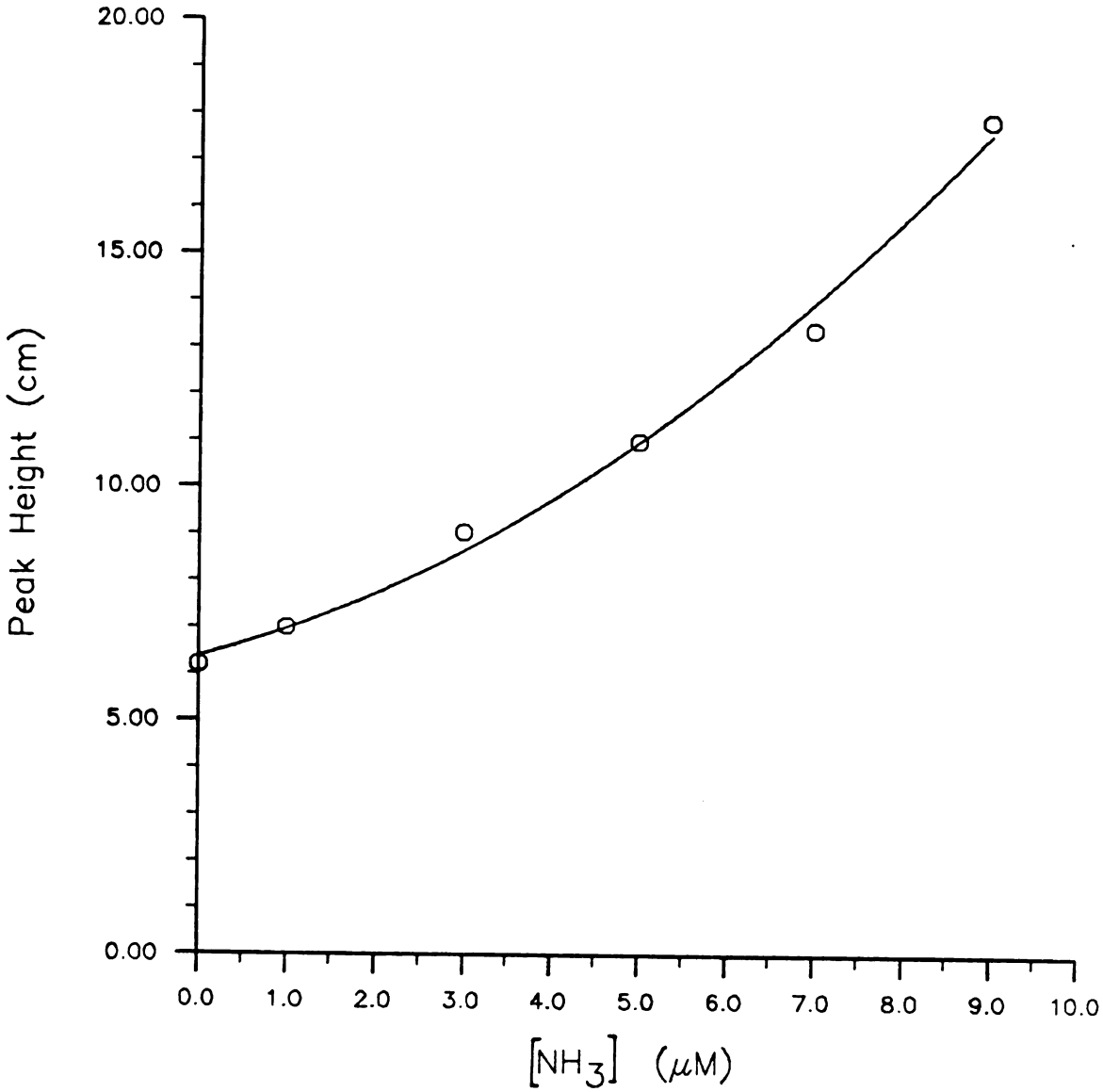

Figure 40. Calibration curve of peak height vs. concentration of ammonia for determination of ammonia in river water by CFA.

VII. CONCLUSION

In any analytical determination interferents can have extremely detrimental effects. Ammonia in its vapor state was diffused across a gas diffusion membrane to remove the interferents. This was achieved with only limited success because of the low concentration of ammonia being detected. To detect these trace levels of ammonia more efficiently a much longer dialyzer with a longer residence time should improve the sensitivity of this system.

In the future, it would be interesting to investigate the actual mechanisms of the interferents. Imidazole, Fe^{3+}, and Ni^{3+} are of particular ineterst because of the nature of their interference.

As a closing remark it should be re-emphasized that FIA is truly easily adapted to suit the requirements of a particular analysis. This CL determination is impossible to perform on a segmented-flow analyzer (CFA) because the sample cannot be mixed with the reagents and introduced into the detector rapidly enough to detect the peak CL signal. Performing this analysis on a stopped-flow instrument has the disadvantage that the ammonia and the hypochlorite must be mixed prior to being measured in the instrument. During this lag time the monochloramine can decompose. Therefore, with only minor modifications to the system proposed it can be easily developed into a fully automatated ammonia analyzer.

LIST OF REFERENCES

LIST OF REFERENCES

1. Leonard T. Skeggs, Am. J. Clin. Pathol. 28, 311 (1957)

2. J. Ruzicka and E. H. Hansen, Flow Injection Analysis, John Wiley and Sons, NY (1981)

3. D. H. Spackmen, W. H. Stein, and S. Moore, Anal. Chem. 30, 1190 (1958)

4. G. Nagy, Z. S. Feher, and E. Dungor, Anal. Chem. Acta. 52, 47 (1970)

5. H. U. Bergmeyer and A. Hagan, Z. Anal. Chem. 261, 333 (1972)

6. Kent K. Stewart, Talanta 28, 789 (1981)

7. V. R. White and J. M. Fitzgerald, Anal. Chem. 44, 1267 (1972)

8. J. J. T. Gerding, H. J. M. Kempen, B. J. M. Lamers, and M. H. Gerding, J. Chromatog. 66, 145 (1972)

9. J. D. Frantz and P. E. Hare, Annual Rept. Director Geophy. Lab. 1630, 704 (1973)

10. P. E. Hare, ibid, 1630, 701 (1973)

11. Z. S. Feher and E. Pungor, Anal. Chem. Acta. 71, 425 (1974)

12. Kent K. Stewart, Gary R. Beecher, and P. E. Hare, Anal. Biochem. 70, 167 (1976)

13. J. Ruzicka and E. H. Hansen, Anal. Chem. Acta. 78, 145 (1975)

14. J. Ruzicka and J. W. B. Stewart, Anal. Chem. Acta. 79, 79 (1975)

15. J. W. B. Stewart, J. Ruzicka, H. Bergamin Filho, and E. A. Zagatto, Anal. Chem. Acta. 81, 371 (1976)

16. J. Ruzicka, J. W. B. Stewart, and E. A. Zagatto, Anal. Chem. Acta. 81, 387 (1976)

17. J. W. B. Stewart and J. Ruzicka, Anal. Chem. Acta. 82, 137 (1976)

18. E. H. Hansen and J. Ruzicka, Anal. Chem. Acta. 87, 353 (1976)

19. J. Ruzicka, E. H. Hansen, and E. A. Zagatto, Anal. Chem. Acta. 88, 1 (1977)

20. E. H. Hansen, J. Ruzicka, and B. Rietz, Anal. Chem. Acta. 89, 241 (1977)

21. J. Ruzicka, E. H. Hansen, and H. Mosbaek, Anal. Chem. Acta. 92, 235 (1977)

22. J. Ruzicka and E. H. Hansen, Anal. Chem. Acta. 99, 37 (1978)

23. Bernard Rocks and Clifford Riley, Clin. Chem. 28, 409 (1982)

24. H. Bergamin, B. F. Reis, and E. A. G. Zagatto, Anal. Chem Acta 97, 427 (1978)

25. D. Betteridge, Anal Chem 50, 832A (1978)

26. J. Ruzicka, E. H. Hansen, and A. Ramsing, Anal. Chem Acta 114, 19 (1980)

27. H. Bergamin, E. A. G. Zagatto, F. J. Krug, and B. F. Reis, Anal. Chem Acta 101, 17 (1978)

28. J. H. M. Van Den Berg, R. S. Deelder, and H. G. M. Egberink, Anal. Chem Acta 114, 91 (1980)

29. G. Taylor, Proc. R. Soc. London Ser A. 219, 186 (1953)

30. O. Levenspiel, Chemical Reaction Engineering 2nd Edition, Wiley, NY 1972

31. R. Tijssen, Anal. Chem Acta 114, 71 (1980)

32. L. R. Snyder and H. J. Alder, Anal. Chem 48, 1017 (1976)

33. L. R. Snyder and H. J. Alder, Anal. Chem 48, 1022 (1976)

34. P. J. Concus, J. Phys. Chem. 74, 1818 (1970)

35. V. J. Levich, Physiochemical Hydrodynamics, Prentice Hall, Englewood Cliffs, New York, p681, 1962

36. Lloyd Snyder, Jacob Levine, Robert Stoy, and Aldo Conetta, Anal Chem 48, 942A (1976)

37. L. R. Snyder, J. Chromatog 125, 287 (1976)

38. L. R. Snyder, Anal Chem Acta 114, 3 (1980)

39. H. O. Albrecht, Z. Phys. Chem. 136, 321 (1928)

40. U. Isacsson and G. Wettermark, Anal. Chem. Acta. 83, 227 (1976)

41. U. Isacsson and G. Wettermark, Anal. Letters 11, 13 (1978)

42. D. F. Marino and J. D. Ingle, Jr., Anal. Chem. Acta. 87, 163 (1976)

43. D. F. Marino and J. D. Ingle, Jr., Anal. Chem. 53, 456 (1981)

44. W. R. Seitz and M. P. Neary, Anal Chem. 46, 188A (1974)

45. Frans Gorus and Eric Schram, Clin. Chem. 25, 512 (1979)

46. U. Isacsson and G. Wettermark, Anal. Chem. Acta. 68, 339 (1974)

47. W. Rudolf Seitz, J. Phys. Chem. 79, 101 (1975)

48. U. Isacsson ,J. Kowalewska, and G. Wettermark, J. Inorg. Nucl. Chem. 40, 1653 (1978)

49. R. T. Balcunias, Ph. D. Thesis, Michigan State University (1981)

50. A. K. Babko and N. M. Lukovskaya, Ukr. Khim. Zh. 29, 479 (1963)

51. R. A. Joyner, Anorg. Allg. Chem. 77, 103 (1912)

52. J. Carrell Morris, J. Phys. Chem. 70, 3798 (1966)

53. M. Eigen and L. de Maeyer, Technique of Organic Chemistry, (Edited by A. Weissberger), Vol. VIII, Part II, 2nd Edition, p 1031, Interscience, NY (1963)

54. Ira Weil and J. Carrell Morris, J. Am. Chem. Soc. 71, 1664 (1949)

55. Robert M. Chapin, J. Am. Chem. Soc. 51, 2112 (1929)

56. Charles J. Patton and S. R. Crouch, Anal. Chem. 49, 464 (1977)

57. Eugene Ratzlaff, personal communication

58. I. M. Kolthoff, E. B. Sandell, E. J. Meehan, and Stanley Bruckenstein, Quantitative Chemical Analysis, 4th Edition, Macmillan, NY, p.852 (1969)

59. CRC Handbook of Chemistry and Physics, Robert C. Weast, ed., CRC Press, Cleveland OH, p. D-186 (1978)

60. Treatise on Analytical Chemistry, Pt. II, vol. 2, I. M. Kolthoff and P. J. Elving, Editors, Interscience NY, (1962)

61. Gretchen Rule and W. Rudolf Seitz, Clin. Chem. 25, 1635 (1979)

62. T. T. Ngo, A. P. H. Phan, C. F. Yam, and H. M. Lenhoff, Anal. Chem. 54, 46 (1982)

63. L. F. Fieser and M. Fieser, Advanced Organic Chemistry, Reinhold, NY, 1961 Chapter 26 pp. 845-851

64. W. R. Seitz and D. M. Hercules, Chemiluminescence Bioluminescence, M. J. Cormier, D. M. Hercules, and J. Lee Editors, Plenum Press, NY, 1973 pp. 427-449

65. J. D. Ingle, personal communication

66. N. T. Bolleter, C. J. Bushmann, and P. W. Tidwell, Anal. Chem. 33, 592 (1961)